Localization and Surveillance under Wireless Sensor Network

Doctoral dissertation submitted by

Debajyoti Biswas

Index No.: 2/19/Maths/26

for award of the Ph.D degree of

JADAVPUR UNIVERSITY

Kolkata 700032, India

Supervisor:

Professor Buddhadeb Sau

Department of Mathematics

Jadavpur University

Kolkata 700032, India

October, 2023

CERTIFICATE FROM THE SUPERVISOR

This is to certify that this thesis entitled "*Localization and Surveillance under Wireless Sensor Network*" submitted by Mr. Debajyoti Biswas who got his name registered on 30.07.2019 for the award of Ph.D. (Science) degree of Jadavpur University, is absolutely based upon his own work under the supervision of Dr. Buddhadeb Sau, Professor, Department of Mathematics, Jadavpur University, and that neither this thesis nor any part of it has been submitted for either any degree/ diploma or any other academic award anywhere before under my knowledge.

Buddhadeb Sau. 03/10/2023

....

(Signature of the Supervisor with date and official seal)

DR. BUDDHADEB SAU
Professor
Dept. of Maths., Jadavpur University
Kolkata - 700 032, INDIA

Dedicated To
All the Living People of the Planet

PREFACE

This thesis is submitted at Jadavpur University, Kolkata 700032, India, for the degree "*Doctor of Philosophy*" in science. The research described herein is conducted under the supervision of Professor Buddahdeb Sau at the Department of Mathematics, Jadavpur University, between the time period February, 2017 and October, 2023.

This research work is original to the best of my knowledge except where the references and acknowledgments are made to the previous works. Neither this nor any substantially similar research work has been or is being submitted for any other degree, diploma, or other qualification at any other university.

Debajyoti Biswas

.....

Debajyoti Biswas

Date: 03/10/2023

Acknowledgment

Foremost, I would like to express my sincere gratitude to my supervisor **Prof. Buddhadeb Sau**, Jadavpur University, Kolkata 700032, for his continuous support of my related study and research. His patience, motivation, immense knowledge, and hard questions incensed me to widen my research from various perspectives. His guidance helped me in all the time of research and writing of this thesis.

I must express my very profound gratitude to *all the teachers of the Department of Mathematics, Jadavpur University* for providing me with unfailing support throughout the years of study and through the process of researching.

I would like to thank *all my fellow labmates* in Jadavpur University, Kolkata, for the discussions and working together before deadlines.

I would like to acknowledge *Council of Scientific and Industrial Research (CSIR)* for giving the financial support in the form of research fellowship to carry out this work.

I would also like to acknowledge **Jadavpur University, Kolkata, India**, and University Grant Commission (UGC), Govt. of India, for the assistance to continue my research work towards the Ph.D. degree.

Flowchart: Localization and Surveillance using WiFi Technology

Input:	WiFi modules plotted in indoor and outdoor.
Output:	WiFi modules programmed with a technique for distance estimation, position localization, vehicle tracking, or indoor surveillance for the application, which are appropriate.

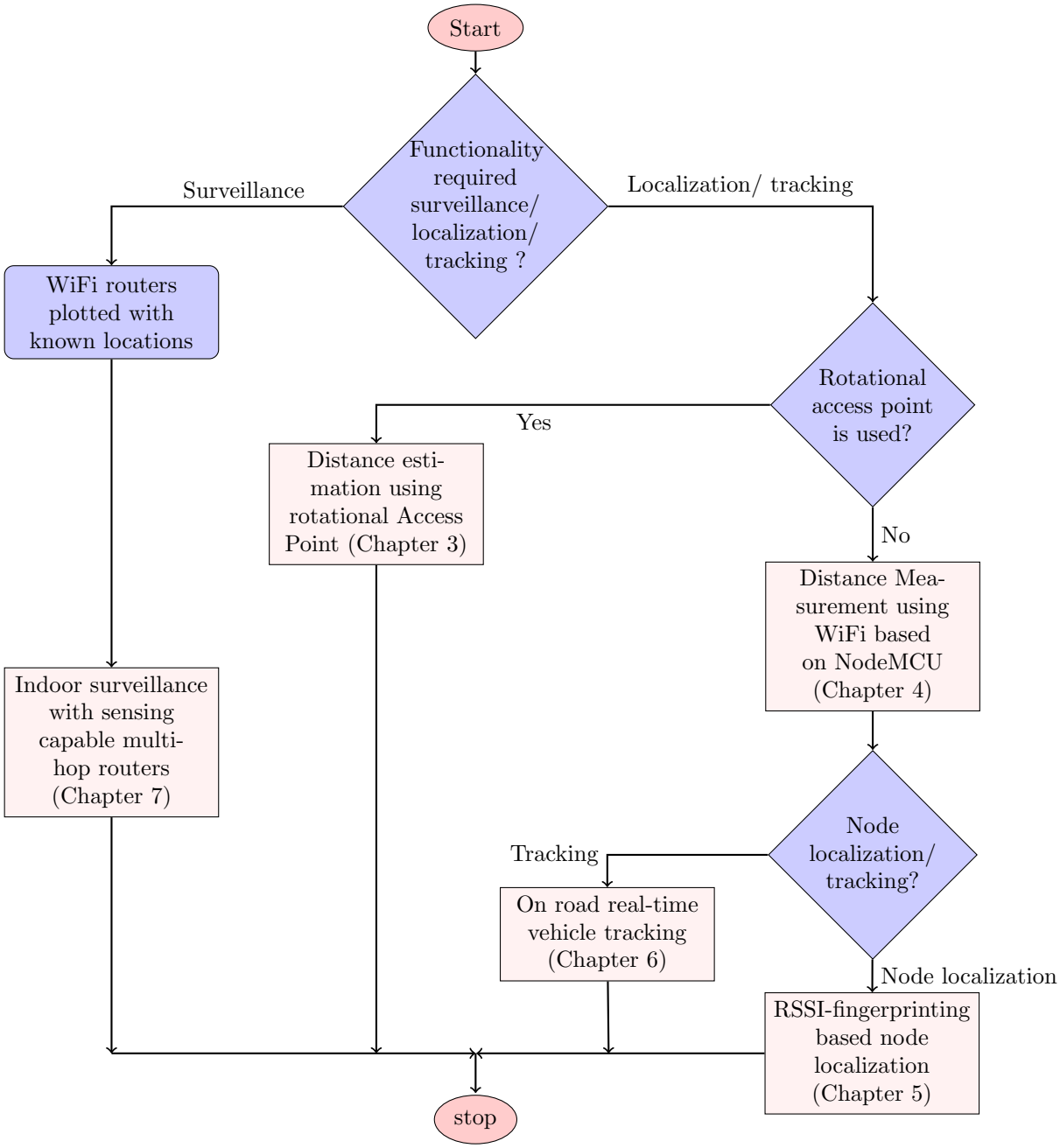

Contents

Chapter 1

Introduction

Localization is broadly used in wireless sensor network (WSN) [23] to identify the current location of the wireless devices. A WSN [14] consists of thousands of devices, and they are connected to each other wirelessly. The wireless connection reduces not only the cost of installation but also maintenance overhead. In wireless technology, Wi-Fi is popular due to its inherent features. Even in the currently appearing Internet of Things (IoT) technology, it is very much suitable. However, due to noise, shadowing, and fading effects on the signal in the environment, it is not easy to estimate the exact location of the wireless device in an environment, specifically in the indoor environment [72]. In addition, the environmental effects repeatedly change from time to time. Therefore, the location of a wireless device using signal strength is important because the data rate and sensing capability entirely depend on it. In particular, manually finding the location of a device is very difficult in a dense network topology [68]. It raises a problem where one must identify the current location of the device without using any special hardware. The signal strength-based localization techniques make the process simple and economical. Therefore, researchers currently focus on the received signal strength indicator (RSSI)-based localization approach [5]. To mitigate the influence of environmental effects in the RSSI technique [95], different methods have been proposed in the literature. However, the existing

methods fail to achieve the desired level of performance in several environments. To overcome such drawbacks, this thesis has proposed some robust localization techniques using Wi-Fi signals under different environments.

In different real applications, the messages may scatter due to various reasons, such as external noise, effects of electronic gadgets, signal blockage, etc. The position-based wireless communication using Wi-Fi [71] is one of the most compelling and demanding techniques to address such issues. In position-based communication establishment between wireless devices, the knowledge of their positions is essential. Communication to the devices with their positions reduces various external effects in communicating signals, including scattering, which not only increases communication efficiency but also reduces processing overhead. By the RSSI-based tracking [49] applications, the trajectory of a moving device can be easily identified. For the long ranges between these devices, the exchange of data may be significantly distracted. Therefore in WSN, a proper communication strategy needs to be developed to limit the scattering of messages.

Typically, a common Wi-Fi router provides service through a one-hop network topology. When communication is required in a particular direction, the coverage increment of a single-hop connection increases power consumption. It restricts the applicability of single-hop networks. Developing a sensing-capable network to cover a large area, multi-hop communications can be used. It decreases power consumption.

This thesis has focused on a different kind of localization and surveillance system based on WSN consisting of Wi-Fi routers. It first has proposed some improved localization techniques to find sensor locations. Then, with these sensors, a multi-hop network is developed to deal with the surveillance system. This thesis also has provided efficient and robust tracking technique in same specific environments.

1.1 Fundamentals of Wi-Fi Technology

Wi-Fi is an alternative network solution to wired networks, which is commonly used for connecting devices in wireless mode. Wi-Fi stands for *Wireless Fidelity*

and is a generic term that refers to IEEE 802.11 standard for wireless local networks (WLANs). Wi-Fi uses radio technology to exchange data at high speed, which commonly operates on a 2.4 GHz radio spectrum within a 30 m range and produces 4-6 Mbps data speed. Wi-Fi may be used for several functionalities in WSN, including communication [11], sensing [56], monitoring [66], and control [21]. Its working modes are described below:

- A Wi-Fi transmitter device [90] transmits data through a radio signal with the help of an antenna to one or more receiver devices [34].

- A Wi-Fi receiver device receives the signal and acquires the data. Then it sends the information to the computer with the help of a wired connection [69] for processing.

The Wi-Fi routers can work as a transceiver together for transmitting and receiving data [84]. Commonly the commercial routers are connected with wired cables to the WLANs and provides access to indoor computers or smartphones through radio signals. A typical diagram of the Wi-Fi infrastructure is shown in Fig. 1.1.

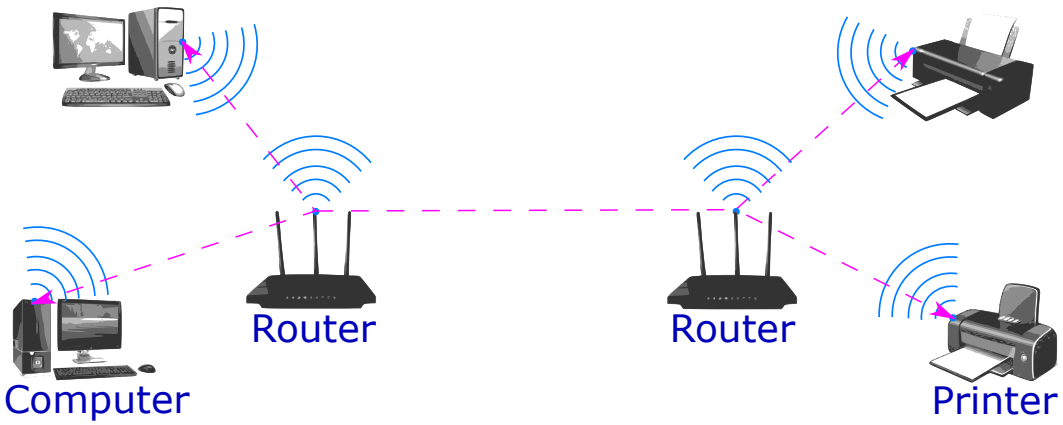

Figure 1.1: A diagram of WiFi System.

1.1.1 Benefits of Wi-Fi

The wireless nature of such a network permits the users to access network resources from any place within the network. Some primitive functionalities described below can be achieved easily by the wireless network using Wi-Fi.

- Mobility: A user can move from one place to another with his personal electronic devices. In a conventional wired network, users cannot access services from different regions with their personal devices due to the limitations of connections. The user can easily move between the different regions with the devices in a wireless network.
- Connectivity: Connectivity stands when two or more devices are able to stay connected with each other. In a wired network [26], it is impossible for the users to remain connected to the network in moving conditions. In Wi-Fi-based scenarios, a user can use network connectivity and communication in moving conditions through the wireless medium.
- Expandability: Wireless networks [100] can adopt and manage a large number of users. A sudden increase in the number of customers can easily be managed with existing equipment, with a suitable software development.
- Cost: The more important thing about a network is its installation and maintenance cost. To serve the wired network connectivity among a large number of users, there must be a huge installation and maintenance cost. In contrast, wireless networks can serve a large number of users with much lower costs than those of wired networks.

1.1.2 Issues and Drawbacks of Wi-Fi

The modern age technology has adopted Wi-Fi technology [67] due to its several advantages. To relax different restrictions over the conventional network, it introduces several drawbacks. Some major drawbacks and issues have been listed below.

- Security: The wired network is highly secured for data communication [2]. Wireless communication involves security threats which becomes an important research area.

- Scalability: The wired network connection can be spread over several kilometers. The standard range of a common Wi-Fi router [81] with traditional equipment is up to 30 m. It is insufficient to serve the users in a distant place. Moreover, wireless signals can be blocked by tree canopies, obstacles, buildings, etc., which prevent reliable communication with distant users. The multi-hop wireless network [77] is a solution to this problem.

- Network speed: The wire connection can provide higher speed (100 Mbps up to several Gbps). The speed provided by a wireless connection [59] (typically 1-54 Mbps) is much slower than a wired connection. Even the signal between two devices can be affected by the surrounding signals present in the environment. Some sophisticated devices with relevant software [41] are necessary to resolve this problem.

This thesis mainly has focused on the scalability of the network. It has developed a localization technique to estimate the location of sensors. It also has developed a method to track vehicles. Our goal is to achieve the above-mentioned services in reality with the help of a large number of sensor nodes or reference devices for a wireless network [98]. Developing a WSN there have mainly two challenges, one is cost and another is energy. To conquer these issues, we have tried to develop a WSN with the help of cheap and energy-saving modules, which are easily available in the market as well as IoT-enabled [65]. In general, multi-hop communication is designed for surveillance with a considerable increase in network coverage with low energy cost. We have implemented a sensor-based indoor surveillance system, where, multi-hop routers are installed in different rooms, and different sensors are associated with them to look after irregular activities in the room such as alcohol, fire, etc. Moreover, by connecting to any router with a smartphone, different irregular activities in a room can be detected by the smartphone's APP. We have designed this APP [1]. It saves a huge amount of energy compared to direct communication.

In this thesis, we mainly focus on three different issues, including indoor localization, on-road vehicle tracking, and indoor surveillance system on the basis of Wi-Fi technology [93]. According to the requirement, some Wi-Fi modules which are easily available in the market are described below.

1.2 Some useful low cost Wi-Fi modules

A module is a part that can be easily added, removed, or replaced in a system. A router consists of different kinds of modules for various purposes, such as sensing, processing, tracking, and communications. This work has considered four Wi-Fi modules to design the WSN system: 1) Node MCU, 2) ESP32, 3) Wemos, and 4) Arduino Uno. The following table shows the parameters based on which the modules can be selected for a specific application.

Table 1.1: Comparison of Node MCU, ESP32, Wemos, and Arduino Uno modules

Modules	Node MCU	ESP32	Wemos	Arduino Uno
Role of the module	Microcontroller development board	Chip on microcontroller development board	Microcontroller development board	Microcontroller development board
Signal propagation	Omni-directional	Omni-directional	Omni-directional	No
Operating voltage	3.3v	3.3v	5v	5v
WiFi	Yes	Yes	Yes	No
Bluetooth	No	Yes	No	No
Coverage	21 m	25 m	18 m	No
Efficiency	Medium	High	Medium	Medium
Price	$5.3	$8.2	$5.5	$7.66

In the market, various sophisticated modules are available, like Jetson Nano, Raspberry Pi, etc. The cost of the Jetson Nano module is $165, and the cost of Raspberry Pi is $175. The above table shows that the modules mentioned above are of much low cost. This thesis has used two or three modules at the same site to develop a router with relevant functionalities having similar performance as the WSN system consisting for Jetson Nano or Raspberry Pi. It reduces the cost

of implementation. The main functions of these modules are briefly described below.

1.2.1 Node MCU

The Node MicroController Unit (Node MCU) (Fig. 1.2) is a development board with Wi-Fi capability. It uses an ESP8266 microcontroller chip. In the localization technique, this module is preferred because of its programming simplicity and low energy consumption property. In the indoor environment, sensors are

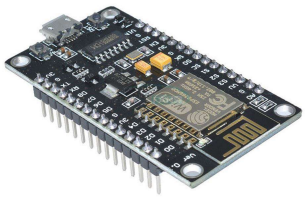

Figure 1.2: Node MCU (ESP8266).

deployed with very short distances among them (i.e., less than 20 m). Therefore, Node MCU is a greedy choice for indoor applications.

1.2.2 ESP32

The ESP32 (Fig. 1.3) development board is a popular system based on the ESP32 microcontroller chip, which supports dual-mode (Wi-Fi and Bluetooth) of communication. It can cover a large area compared to Node MCU. A vehicle

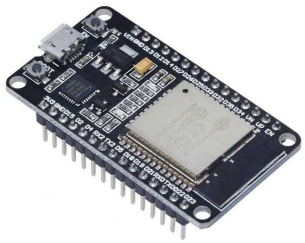

Figure 1.3: ESP32.

tracking system inherently requires a comparatively large area. Therefore, the use of ESP32 is popular in vehicular tracking.

1.2.3 Wemos

The wemos D1 R2 (Fig. 1.4) is a development board with Wi-Fi functionality. It consists of the ESP8266 microcontroller chip. Its coverage range is about 15 m,

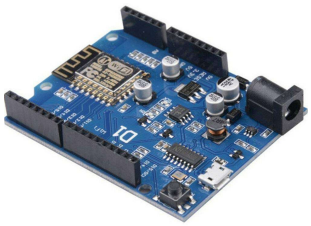

Figure 1.4: Wemos D1 R2 ESP8266.

which is very useful for indoor communication. Its operating voltage is 5v.

1.2.4 Arduino Uno

Arduino Uno (Fig. 1.5) board is an open-source electronics platform based on easy-to-use software. It doesn't have built-in Wi-Fi or Bluetooth facilities. It

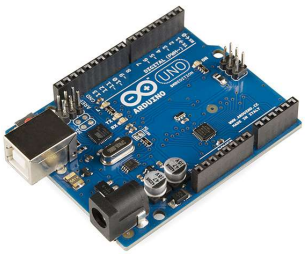

Figure 1.5: Arduino Uno.

operates on 5v. Since Arduino Uno originally has no wireless capability, it is very useful for wired sensor connections. However, external Wi-Fi or Bluetooth antenna needs to be separately included to enable its wireless capability. To make

a multi-hop router network, for sensor data management tasks Arduino Uno is a suitable option.

Note that both the NodeMCU, ESP32, wemos D1 R2 and Arduino Uno can be programmed by Arduino integrated development environment (IDE) software. To perform different types of work with these modules, it requires different types of programs. According to the program, they have different functionalities, which restrict the module to be used in practical applications. The work categories of these modules regarding the program are described below.

1.3 Mode of module

A module may be used to play the role of an access point (AP), a station (STA), or a controller. Fig. 1.6 describes the router framework consisting of three modules:

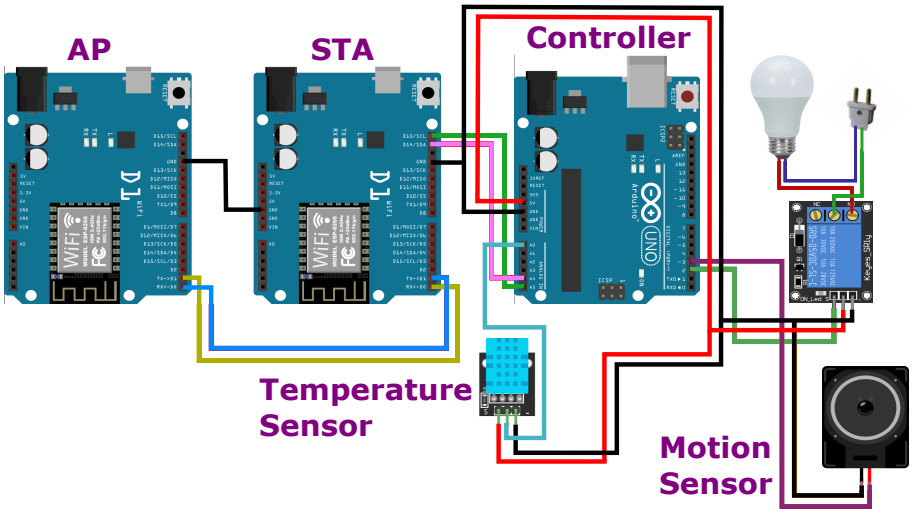

Figure 1.6: Router framework.

1) AP, 2) STA, 3) controller based on Wi-Fi functionalities. These three modes of action of a module are described below.

1.3.1 Access Point

As a standalone wireless module, AP is an integral component of the router itself. Its main work is to allow other wireless devices to connect to the network and data forwarding. The AP decides the next-hop router for data forwarding according to the routing protocol. The data will be sent to the next-hop router via wireless connection. The AP receives data from the connected sensor devices or forwarding data from other routers. The AP may receive two types of data : 1) query for some information from a specific router sensed by connected sensors, 2) forwarding data from another router. If it receives query then the AP will send it to the controller via STA for required data sensed by the connected sensors devices. The response will not forwarded to AP to STA through wire, inside the router. The response will forwarded from STA of a router to AP of another router wirelessly through a different path. The AP receives forwarding data via the STA as the response against the query, and data directed towards the destination. In either case, the data with will be forwarded to the next-hop according to the routing protocol. To perform such work, the module AP has been programmed accordingly. Different types of AP modules are required for different purposes. For indoor localization a Node MCU, for vehicle tracking an ESP32, and for multi-hop router network a wemos may be used as an AP.

1.3.2 Station

A station (STA) is a module which is an integral component of the router along with the AP. The main work of STA is that it connects to the AP of other routers to increase network coverage. It receives data collected by the AP of same router through wire connection and sends it to the AP of the destination router through wireless connection. It cannot connect more than one AP at a time. For establishing connectivity between two modules, an STA is also required along with the AP. The module for designing the STA has to be of the same type (ESP32 or wemos) as that of the AP. For indoor localization a Node MCU, for vehicle tracking an ESP32, and for multi-hop router network a wemos may be

programmed as the STA.

1.3.3 Controller

A controller is a module that manages or directs the flow of data between two systems (e.g., sensors and STA). In the router, it is used to exchange data between STA and sensors through wires. The controller is programmed to manage and forward the sensors data to the STA. In a router, a controller reduces the working burden to the AP and STA, which is connected with wires because with the wire more protected data can be passed than wireless. Arduino Uno is used as controller to communicate between STA and sensors.

1.3.4 Working Procedure

The router consists of wire-connected modules AP, STA, and controller. Both the modules AP and STA can receive and forward the data through communication channels. AP allows other wireless devices (like smartphones, laptops, etc.) to connect to the router, and STA can wirelessly connect to the AP of another router to increase the network size. By connecting multiple routers wirelessly, a multi-hop sensor network can be formed. Fig. 1.7 described the communication strategy of the multi-hop router network, where each router consists of an AP and an STA for communicating with other routers. The STA connects other routers' AP wirelessly to form a network where inside a router, AP and STA communicate with each other using the wired protocol. At a time, an STA can only connect to a single AP, but multiple STAs can be connected to an AP. Whenever an AP or STA module receives data, it forwards it to the connected modules, whether the connected module is the wire or wirelessly connected. However, in the reality, finding the position of a mobile device or static object is important. Using the multi-hop network, it may be solved easily. With the Node MCU modules, the localization framework is designed.

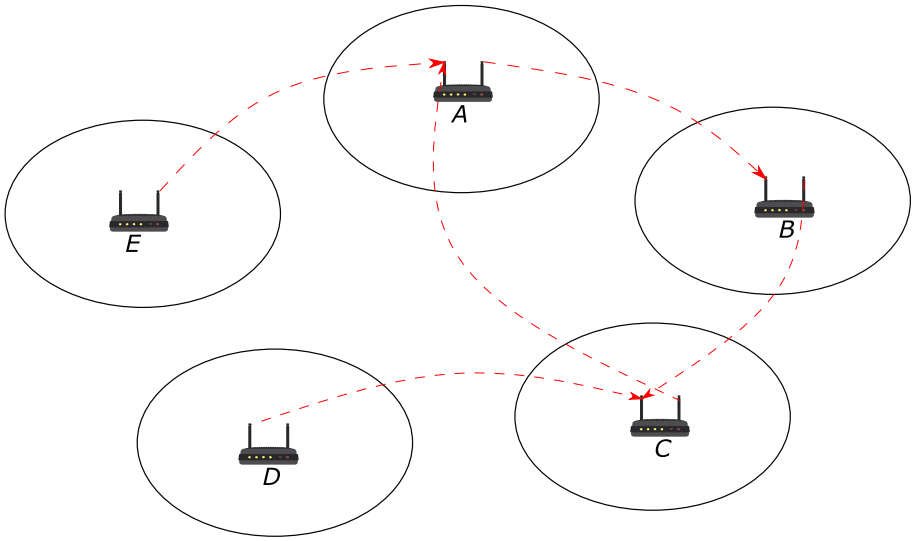

Figure 1.7: Working Procedure.

1.4 Localization

Localization is very crucial information to find the location of the module with the help of a specific method. The information from the module is useless if there is no idea of geographical locations. A wireless network consists of a large number of modules that make the localization procedure more complicated. Moreover, wireless signals are uncertain and vary according to the environment. To overcome such drawbacks, in the literature, various methods have been presented. Such as the trilateration localization method (TLM) [63], where at least three anchor devices are required to locate the position of an unknown device. This localization process is based on the intersecting coverage zones of anchor devices. If the number of anchor devices is increased, then computational and management overhead also is increased, which consumes high energy, leading to serious pricing issues. The angle of arrival (AoA) [24] methods are utilized with delays, and angle measurement, which is a too lengthy process because of the complexity of the method. The process is time-consuming and needs some additional hardware for computations, which is too costly as well as requires extra overhead. Those methods are either based on expensive hardware or time-consuming. Among the

localization methods, the most reliable and inexpensive method is the RSSI-based technique. In this work, a simple and robust RSSI-based localization method has been presented to find the location of STA with the help of APs signals in the indoor environment. Though RSSI-based localization methods have some drawbacks, which are described below.

Drawbacks in RSSI-based Localization Techniques:

- Due to the presence of environmental catalyst factors, the measured RSSI values frequently fluctuate, which highly affects the localization method. Because of this fluctuation in RSSIs, the shape of RSSIs are uncertain. So does not represent any pattern significantly.
- Since, due to the signal uncertainty, the RSSI values frequently fluctuate to consecutive positions. Therefore, a proper model with appropriate RSSIs is required to achieve higher accuracy because accuracy depends on the estimated method and the choice of the proper RSSI data.

To mitigate the issues in signals and existing methods, some procedures are taken into consideration, which is described in the following.

Improvement in RSSI-based Localization Techniques:

- In [63], a solution has been proposed with at least three anchor devices, which increase computational overhead as well increase the cost of the system. To reduce the management overhead and overall cost of the system, in this work, at most, two APs are used to localize the location of an STA.
- In [24], the AOA-based localization system is designed with additional expensive hardware, but our proposed work does not use any additional hardware for RSSI-based localization, where the system is designed with a simple setup.
- To get higher accuracy in localization, some special RSSI-based algorithm is used, which is very simple and robust than other state-of-the-art algorithms [63], [24], [38].

To represent the fluctuating character of RSSI data, this work mainly focuses on the least square-based non-linear regression technique, where an exponential model is used to represent the relationship between RSSIs and distances such that monotonic locations can be estimated with the exponential model. Compared to the linear Kalman filter method (KFM) [38], the non-linear exponential model achieves higher accuracy in representing the relationship between RSSIs and distances.

1.5 Vehicle Tracking

Tracking aims to identify the location of a vehicle over time. For example, the trajectory of a vehicle may be tracked. A tracking method also faces a similar challenge as that of localization. Due to mobility, the challenges vary over time. Consequently, sophisticated localization finding methods can not be used.

The camera-based surveillance approach is very costly and may violate the privacy of people. Multi-hop network may be used to improve the performance of tracking mobile objects. This thesis has proposed a simple and robust technique of finding the location for tracking a mobile object. This work mainly has used, a wireless multi-hop router network with the Wesmos D1 R2 and Arduino Uno for indoor surveillance and tracking. The proposed surveillance system is fully sensor based and does not violate user privacy.

It provides almost accurate location in tracking process even when the distances are noisy due to noise in the signals.

1.6 Multi-hop Networks

Multi-hop wireless connections use two or more wireless hops to transmit information from a source to the destination. Without increasing the sensing coverage of an individual router, the connection range of the network can be increased. It reduces the hardware implementation cost. Fig. 1.8 depicts a multi-hop router network scenario with four routers. Each of the routers have the same sensing

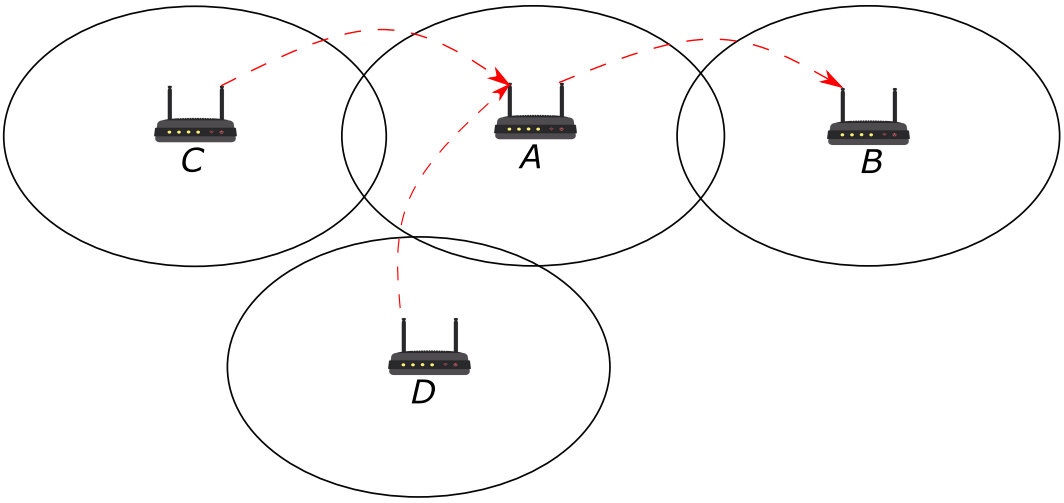

Figure 1.8: Multi-hop router network.

coverage. As mentioned earlier, the STAs of multiple routers can establish connection to the AP of a router, whereas the STA of a router can connect only to a single AP. The common network infrastructure is based on wired cables to produce better network performance and reliability. Fig. 1.9 illustrates conventional wired network scenario, where service may be provided to different buildings by the underground wire connection.

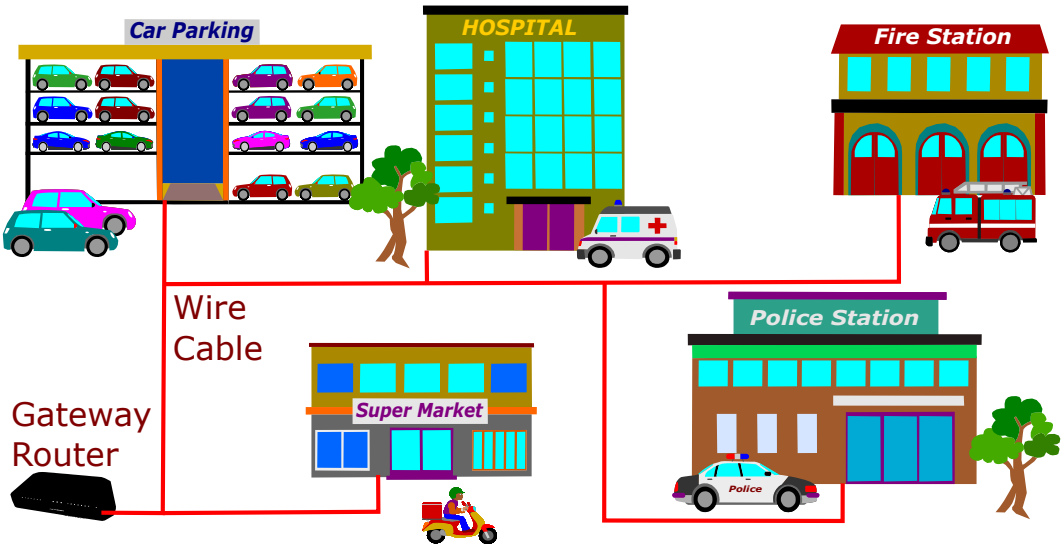

Figure 1.9: Conventional network.

The conventional wired network has some drawbacks, which are described below.

Drawbacks of Conventional Network: Most of the parts of conventional wireless networks are consist of wire cables to produce a high data rate. It may not be useful for several small and personal network systems due to the following reasons:

- wire connections are costly,
- power consumption is very high,
- maintenance is also very expensive.

These issues can be addressed effectively by a wireless multi-hop network.

Advantages of Multi-hop Wi-Fi Network: In the multi-hop wireless network, the modules are lightweight and inexpensive. So it is highly acceptable in some working fields due to the following reasons.

- A wireless router is easily portable from one place to another.
- Multi-hop routing increases communication coverage to any direction.
- Maintenance and installation costs are very low.
- Load can be distributed among multiple routers easily.

The goal of developing the multi-hop network is to satisfy the following properties:

- Cost-effectiveness of the system,
- Energy-efficiency of the system,
- Short communication coverage,
- Capability of multi-hop routing.

To achieve this goal, this thesis has proposed a wireless multi-hop router network for the surveillance system in the indoor environment. The main contributions are described as follows:

- Each router is designed with an AP, an STA, a controller and different sensors depending on applications environment,
- A application (APP) has been designed for providing command and request for real-life use on mobile devices.

1.7 Organization and Scope of the Thesis

This thesis aims to improve the existing technologies of object tracking and surveillance. With this motivation, the thesis has proposed a simple and robust localization technique. This localization is suitable for tracking mobile objects in reality. Using such localization methods a surveillance system has been developed using a multi-hop wireless network.

- In chapter 3, with the angular technique, the distance between the rotating object and the wall is estimated with the help of at most two STAs inside a room. The STA is placed at different angles with the AP, but the AP is fixed to the center of the rotating object. With the intersecting points of two circles generated by the angle, the distance between the wall and the center of the rotating object is estimated.
- In chapter 4, linear distances between the station and access point are estimated using the RSSI technique, where the different experimental environment is considered. With the low-cost modules and simple setup, we have successfully measured the distances between two modules using a wireless signal in a robust manner.
- In chapter 5, the RSSI-based smartphone localization system has been developed for indoor environments, where the smartphone location is determined by the distances of noisy environments. The proposed method is

simple and robust, which produces higher accuracy compared to other existing methods present in the literature.

- In chapter 6, the received signal strength (RSS)-based real-time on-road vehicle tracking infrastructure has been developed where using the RSS from a vehicle to different BSs, vehicle location is determined. This proposed method is very effective for the vehicle tracking system and can produce very prompt responses on vehicle position.

- In chapter 7, an indoor surveillance system has been developed with the multi-hop router network, where the routers are sensing capable and the sensors can control or monitor using a user smartphone. The proposed sensing capable strongly connected multi-hop network is very effective and can do several jobs.

1.8 Conclusions

In this thesis, localization and a tracking system have been designed. Besides, a multi-hop router network has been developed. In the localization system, using the regression technique, with the three APs's distance position of smartphone is localized. For localization, Node MCU modules have been used, which is low cost and efficient. The Node MCU has Wi-Fi functionality, therefore compared to other relative wireless technology its performance is very high. So a better performance can be achieved. Besides, for vehicle tracking, the ESP32 modules can be used, which have more communication range than Node MCU. For vehicle localization, to get higher efficiency, probability-based methods are used. Then, a multi-hop router network is developed with the wemos D1 R2 and Arduino Uno. The router is capable of sensing the environment with the associated sensors.

Chapter 2

Related Work

In this chapter, we present a brief survey of localization, tracking and multi-hop communication techniques and discuss common issues.

2.1 Localization technique

In the localization technique, the related work are as follows.

2.1.1 Literature Survey

Xie *et al.* [82] propose an improved Spearman distance-based KNN (SD-KNN) algorithm. To mitigate different radio terminal effects on absolute RSSI values, rankings are used to replace the absolute ones for position determinations. The Spearman rank correlation coefficient is a non-parametric measure of statistical dependence which evaluates how well the relationship between two variables can be expressed by a monotonic function that is appropriate for both continuous and discrete variables. This localization procedure has been built with an offline fingerprint database. First, the position fingerprints of the objects are collected, then the Spearman distances are calculated to select all locations with a minimum one using the KNN approach. Simulation results demonstrate that the

SD-KNN method outperforms the original KNN method as well as the polynomial regression method under the indoor environment in severe multipath fading. Hoang *et al.* [33] present a soft range limited KNN (SRL-KNN) localization fingerprinting algorithm. Unlike the conventional KNN methods, SRL-KNN scales the fingerprint distances by a range factor associated with the physical distances between the previous and reference positions in the database to mitigate the location ambiguity. The experiment is conducted with the support of an autonomous robot such that the time consumption and the degree of human involvement can significantly be reduced such that the target location navigation and fingerprint collection can be done automatically. The SRL-KNN does not require the knowledge of exact moving speed and direction. Actual on-site experimental results demonstrate that the new algorithm achieves higher localization accuracy compared to other conventional algorithms under the same test environment. Yin *et al.* [88] address the Bayesian sensor fusion technique for distributed position estimation. Where the RSSI-based system is studied using the unscented Kalman filter (UKF) approach for each radio sensor to spatial estimation and proposes a novel distributed method that combines the soft outputs sent from selected sensors as well as computes the appropriate Bayesian estimates at the original positions. The objective is to investigate the probabilistic sensor fusion strategies for position estimation by developing a novel distributed UKF (Distr-UKF) scheme. The approximated inference is sent to the fusion center, which calculates the fused location of the moving object. The computational cost of this algorithm is less and achieves higher accuracy than the centralized UKF method. In [86], an enhanced min-max with area partition strategy (Min-Max-APS) is presented to acquire a better localization performance where the area of interest is first partitioned into four subareas, each of which contains a vertex of the actual area. After, a minimum range difference criterion is planned to determine the target affiliated subarea whose vertex is nearest to the target node for estimating the location. Due to the smaller size of the target affiliated subarea than the actual area of interest, the weighted centroid of the target subarea is more accurate compared to the original ones. Simulation results confirm that the localization errors of the Min-Max-APS algorithm are less than one-half of the extended Min-

Max (E-Min-Max) algorithm and one-seventh of the original Min-Max algorithm. Reference

The existing challenge on localization are describe as follows.

2.1.2 Existing Issues

By reviewing the existing literature, we recognize that some of the issues still need to solve to develop an optimized RSSI fingerprint localization technique. The extracted drawbacks from these articles are listed below:

1. The utilization of a large number of radio devices can mitigate the system's capabilities.
2. The weak signal strength from some wireless devices can reduce the desired performance requirement.
3. The expensive devices can increase the installation cost and maintenance cost significantly.
4. The pre-assuming measurement parameters cannot always produce a good precision.

2.2 Tracking method

In the tracking system, the related work are as follows.

2.2.1 Literature Survey

The vehicular network for current positioning heavily depends on GPS enabled devices [62]. Besides, the angle of arrival (AoA) methods are utilized with delays and angle measurements [47]. Reference [63] introduces a trilateration positioning system (TPS) where three anchor devices are used to localize the position of

unknown devices inside their intersecting coverage zones. In [45], a hunter-prey scenario has been studied where followed prey transmits the signal, and the hunter receives the attenuating signal intensity.

2.2.2 Existing Issues

By reviewing the existing literature, we recognize that some of the issues still need to solve to develop an optimized RSSI based tracking method. The extracted drawbacks from these articles are listed below:

1. The GPS signal can be blocked by tree canopies and obstacle buildings in the central urban areas.

2. For GPS-enabled sensors, there are tremendous pricing as well as energy consumption issues.

3. The AoA methods are time-consuming due to the complexity of the process and need some additional hardware.

4. In TPS, large number of anchor devices always increase the system complexity, energy consumption, and processing overhead.

2.3 Multi-hop Networks

In the multi-hop network, the related work are as follows.

2.3.1 Literature Survey

Reference [43] considers scenarios where only a limited networking infrastructure is available, but a large number of internet of things (IoT) devices are deployed in building a multi-hop ad hoc network to deliver source data to the destination.

This work shows that the actions that the IoT devices take from its policy are determined as to activate or inactivate its transmission. This solution builds a network with higher network performance than the current state-of-the-art solutions in terms of system goodput and connectivity ratio. In [78], to overcome information leakage and increase transmission reliability, a multi-hop relaying strategy is deployed against the unmanned aerial vehicle (UAV) surveillance. The aim is to optimize the throughput by carefully designing the parameters of the multi-hop network, including the coding rates, transmit power, and required number of hops. In the secure transmission scenario, the expressions of the connection probability and secrecy outage probability of an end-to-end path are derived and the closed-form expressions of the optimal transmit power, transmission and secrecy rates under a fixed number of hops are obtained. Simulation shows the impact of network settings on transmission performance. In [44], a quality of experience (QoE) enhancement routing (QER) protocol is designed based on smart collaborative theory. First, crucial parameters which affect data transmission process are analyzed comprehensively and applications of MWN are introduced. Second, two stages of QER protocol, i.e. collaborative perception and smart decision, are designed to collect real-time network information and decide the optimal routing mechanism, respectively. Third, we integrate three routing mechanisms into QER and conduct a comparative analysis. Performance validation demonstrates that our solution is able to intelligently execute the suitable strategy. Reference [32] concurrently considers simultaneous wireless information and power transfer (SWIPT) and routing selection in multi-hop energy-constrained wireless network (MECWN). To reduce energy consumption, first formulate the information and energy allocation problem of link in a forwarding path, which is dependent on the next-hop node, and solve it by an iterative allocation algorithm. The performance studies demonstrate that the algorithms can effectively exploit those node resources whose energy are not enough and significantly decrease the energy consumption.

2.3.2 Existing Issues

The review of the present literature shows that although the methods are effective. However, there still present some drawbacks which restrict their performance.

1. When multiple source nodes deliver their data simultaneously for the destination, there will create some chaos in optimum path selection.
2. Increasing the throughput by improving network parameters, there will require expensive hardware and software.
3. If in a network, each node is connected with more than one node, then the computational complexity and delays increase in data forwarding.

This chapter reviews all those issues to successfully present potential solutions using various new strategies.

Chapter 3

Distance measurement between a Rotational Object and a wall

In this work, a distance estimation procedure between a rotational object and a wall (Fig. 3.1) has been presented. An access point (AP), and two stations (STAs) have been used in this procedure. An AP is a wireless module that allows other wireless modules to connect it. An STA is a module that has the capability to use the network interface by connecting to the AP. The AP [52] is placed on a blade of a rotating object (Fig. 3.2), and from the center of the rotating object, the shortest distance of the wall is estimated. To estimate the shortest distance between the center of the rotating object and wall, at least two STAs [94] are required. The blades of the object rotate; therefore, the distance of the AP from STA has the minimum distance and the maximum distance. The distance can be calculated by any technology such as RSSI, etc. Moreover, the position of the STA may be in different locations [31] on the wall but not on the same vertical line. Firstly, we estimate a distance and angle, i.e., the distance between an STA and the center of the rotating object and the angle between a vertical line passing through an STA and the line joining the STA and the center of the rotating object. Using the angle and distance, we will get a cone capturing both sides of the wall. If we neglect the thickness of the wall and keep the two STAs in different positions

(not on the same vertical line) on the same plane (wall), then two circles of two cones will intersect each other. The intersection points lie on both sides of the wall, and half of the distance between the two intersecting points is the original shortest distance between the wall and the center of a rotating object.

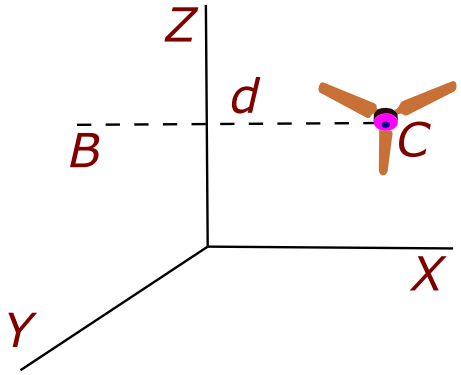

Figure 3.1: Perpendicular distance of the center of a rotating object and a wall.

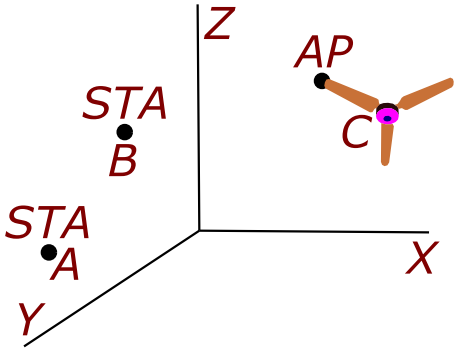

Figure 3.2: Positions of the AP and STAs.

3.1 System Model

Consider the scenario of a room where a rotating object is rotating above the horizontal plane and parallel to the horizontal plane. The room is square-shaped and has complete empty space such that the line of sight (LoS) signal [60] can propagate in every direction. Here, the signal propagations between two modules [6], i.e., AP and STA, are considered. From AP, the signal propagates to STAs,

and the STAs are placed at different locations to receive the signal. Both AP and STA have an isotropic antenna. Therefore, the omnidirectional signals are radiated from them. If the AP is in the center of the rotating object, then the distance between the AP and the STA will remain constant (Fig. 3.3).

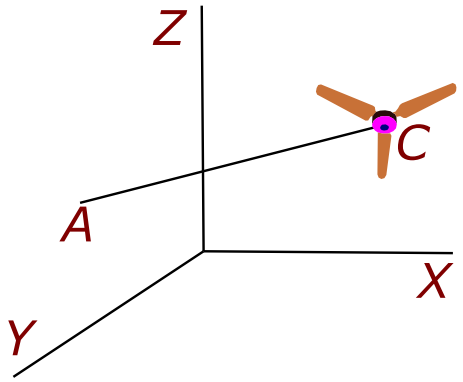

Figure 3.3: AP is in the center of the rotating object.

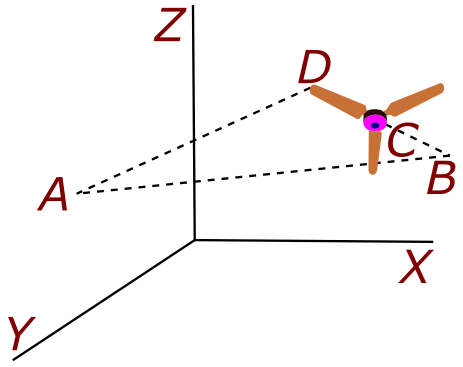

Figure 3.4: AP is in the blade of the rotating object.

In this way, we need the STA to find the perpendicular distance between the rotating object and the wall. But if we put the AP on a blade of the rotating object, more than one distance can be measured (Fig. 3.4), and we will achieve our goal using two STAs only instead of three STAs. The AP is placed on a blade of the rotating object. For the rotations of the object, the angle between AP and STA, as well as their intermediate distances, are repeatedly changed. Since the room is square-shaped, thus the signal propagation on every side is the same. So, only one side out of four sides can express the changing behavior of the signal

due to rotation. Therefore, we choose a side where the STA is kept on the wall at different positions [16].

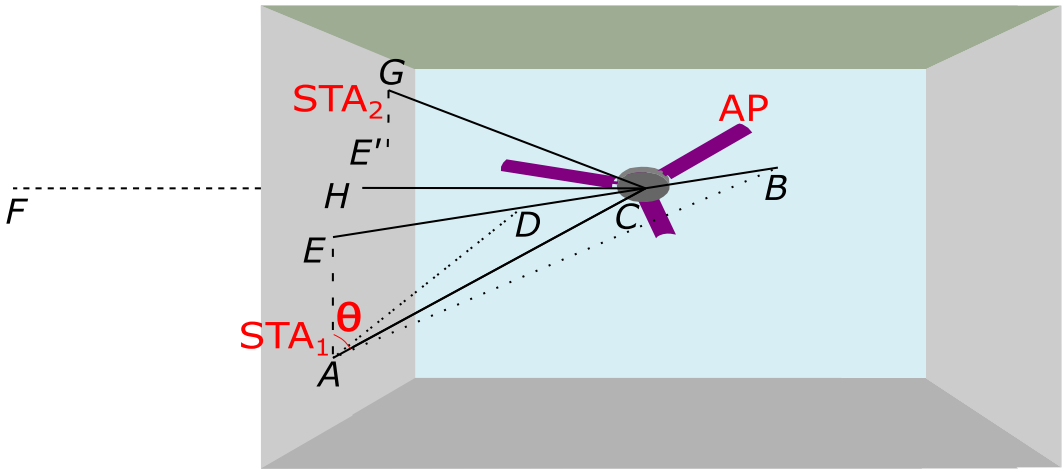

Figure 3.5: Positions of STA inside the room, in the wall, where FH indicates the image distance between center of the rotating object and the wall.

Fig. 3.5 shows the scenario where two positions of STAs are considered on the wall. The AP is at a blade, and the STAs are placed in the respective positions A and G. The angle of $\angle EAC$ is θ. FH is the image distance between the wall and AP. Since the rotating blade covers a 360° angle during its rotation, where AP's minimum distance is AD, and the maximum distance is AB from the STA_1. The distance of FC is $d^{'}$ and the distance of $FH = HC$ is d.

3.2 Mathematical Model

Consider a room where an STA is placed on a wall. The angle between the vertical line passing through STA and the line which passes through STA and the center of rotating object is θ. Let the position of the STA is A and the position of the center of the rotating object is C, and the horizontal distance of C from this wall and perpendicular to the vertical line passing through A is $\overline{\text{CE}}$, where E is the position in the wall. Let the radius of the blade be r, i.e., $\overline{\text{CD}} = \overline{\text{CB}} = r$. The maximum distance between STA_1 and the blade is $\overline{\text{AB}} = d_{max}$ and the minimum

distance between the fan blade, and STA_1 is $\overline{\text{AD}} = d_{min}$, where $\overline{\text{BD}} = 2r$. We want to find the $\theta = \angle EAC$ (Fig. 3.6).

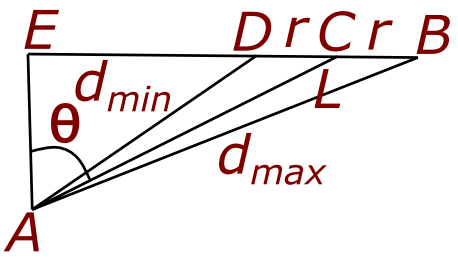

Figure 3.6: Measurement background.

Consider $\triangle ACE$ where the sum of the internal angle is $\angle EAC + \angle ACE + \angle CAE = \pi$. The angle $\angle CEA = \frac{\pi}{2}$. Therefore, $\angle EAC + \angle ACE + \frac{\pi}{2} = \pi$. So, we can write that,

$$\angle EAC = \frac{\pi}{2} - \angle ACE \tag{3.1}$$

Consider $\triangle ACD$, $\angle ACD + \angle CDA + \angle DAC = \pi$, as $\angle ACD = \angle ACE$, thus, $\angle ACE + \angle CDA + \angle DAC = \pi$, we can write that,

$$\angle ACE = \pi - \angle CDA - \angle DAC \tag{3.2}$$

Substituting (3.2) into (3.1) we get $\angle EAC = \frac{\pi}{2} - \angle ACE = \frac{\pi}{2} - \pi + \angle CDA + \angle DAC = \angle CDA + \angle DAC - \frac{\pi}{2}$. The AC is the median of $\triangle ABD$ at $\overline{\text{BD}}$ from A. Now, using the formula of the length of a median when the length of three sides of a triangle are given, $L = \overline{\text{AC}} = \frac{\sqrt{2\overline{\text{AB}}^2 + 2\overline{\text{AD}}^2 - \overline{\text{BD}}^2}}{2} = \frac{\sqrt{2{d_{max}}^2 + 2{d_{min}}^2 - 4r^2}}{2}$.

Consider $\triangle ACD$, using the properties of triangles we can get,

$$cos(\angle DAC) = \frac{\overline{\text{DA}}^2 + \overline{\text{AC}}^2 - \overline{\text{CD}}^2}{2 \times \overline{\text{DA}} \times \overline{\text{AC}}} = \frac{{d_{min}}^2 + L^2 - r^2}{2 d_{min} L} \tag{3.3}$$

Also,

$$cos(\angle CDA) = \frac{\overline{\mathrm{CD}}^2 + \overline{\mathrm{DA}}^2 - \overline{\mathrm{AC}}^2}{2 \times \overline{\mathrm{CD}} \times \overline{\mathrm{DA}}} = \frac{{d_{min}}^2 - L^2 + r^2}{2rd_{min}} \tag{3.4}$$

Thus we can get,

$$\angle EAC = cos^{-1}(\frac{{d_{min}}^2 - L^2 + r^2}{2rd_{min}}) + cos^{-1}(\frac{{d_{min}}^2 + L^2 - r^2}{2d_{min}L}) - \frac{\pi}{2} \tag{3.5}$$

The angle estimation procedure has been described in the following.

For getting almost exact d_{max}, d_{min} we have to take a lot of d_is. If the degree of angle of rotation between two consecutive reading is relatively prime to 360, then it will be possible to get d_is of 1° interval.

Algorithm 3.1 Angle Estimation

1: **procedure** ESTIMATION OF ANGLE OF THE CENTER OF CEILING FAN WITH THE STA
2: **Input:** $d_i \longleftarrow$ distance of AP from the STA, $i = 1, 2, \ldots, n$;
3: $r \longleftarrow$ radius of the rotating object;
4: **Output:** θ estimated angle of the center of ceiling fan with the STA;
5: Find the maximum and minimum value among $d_1, d_2, \ldots, d_n$;
6: Define $d_{max} = max\{d_1, d_2, \ldots, d_n\}$, and $d_{min} = min\{d_1, d_2, \ldots, d_n\}$;
7: $L = \frac{\sqrt{2{d_{max}}^2 + 2{d_{min}}^2 - 4r^2}}{2}$;
8: $\theta = cos^{-1}(\frac{{d_{min}}^2 - L^2 + r^2}{2rd_{min}}) + cos^{-1}(\frac{{d_{min}}^2 + L^2 - r^2}{2d_{min}L}) - \frac{\pi}{2}$;
9: **end procedure**

Let the room be XYZ space. We consider the AP is rotating $\parallel$ to XY plane. Using the distance between the center of rotating object and STA, and the angle, we can find a circle (Fig. 3.7).

This circle is the probable position of the AP with respect to the STA. The circle lies on the plane containing AP $\parallel$ to XY plane. The center of the circle lies at the intersection of plane passing through AP and $\parallel$ to XY plane and the line passing through STA $\parallel$ to the Z axis. The radius of the circle is the shortest

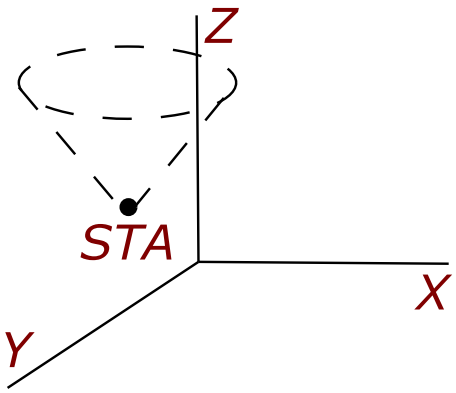

Figure 3.7: One STA scenario.

on the distance of the center of the rotating object containing AP from the line passing through STA and $\|$ to the Z axis. If there are two STAs, then there will be two circles (provided the STAs don't lie on the same Z axis) (Fig. 3.8).

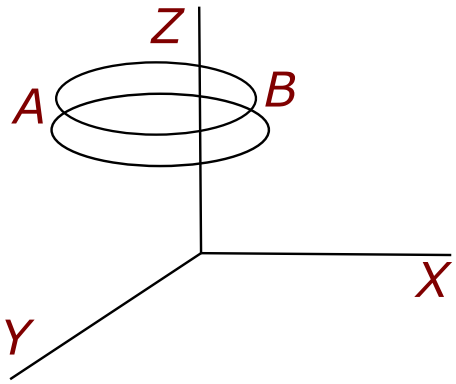

Figure 3.8: Two STAs scenario.

Two intersection points of two circles will be the probable two points of the AP. One is real, and another is a mirror image with respect to the wall. But we want the distance of AP from the wall. Then we calculate the midpoint of the intersection point. Then we have to find the distance of any intersection point from the midpoint, i.e., half the length of distance between two intersection points (Fig. 3.9).

The distance estimation procedure has been describe in the following.

Algorithm 3.2 Distance Estimation

1: **procedure** ESTIMATION OF THE PERPENDICULAR DISTANCE BETWEEN THE CENTER OF THE ROTATING OBJECT AND A WALL

2: /* Let two STAs STA_i for $i = 1, 2$ on the same wall and in different Z ordinate */;

3: **Input:** $L_i \longleftarrow$ distance between center of rotating object containing AP and STA_i, $i = 1, 2$;

4: $\theta_i \longleftarrow$ angle between the line passing through STA_i, parallel to Z axis and the line joining the centre of rotating object containing AP and the STA_i on wall, $i = 1, 2$;

5: $(x_i, y_i, z_i) \longleftarrow$ coordinate of the STA_i on wall, $i = 1, 2$;

6: **Output:** $d \longleftarrow$ estimated distance;

7: /* Consider two cones $S_i, i = 1, 2$ with vertex (x_i, y_i, z_i), axis $\parallel$ to Z axis */;

8: Find the equation of circles (C_i) which are the base of cone S_i, angle of inclination θ_i, slant height L_i for $i = 1, 2$;

9: Compute intersecting points (P_1, P_2) for the pair of circle C_1, C_2;

10: Compute $d = \frac{d^{'}}{2}$;

11: /* $d^{'} \longleftarrow$ is the distance between P_1 and P_2 and d is the distance between AP and the wall */;

12: **end procedure**

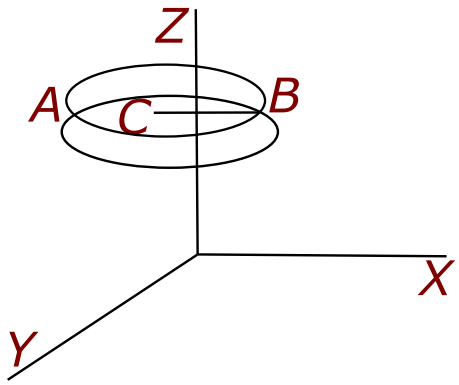

Figure 3.9: Intersection of two circles.

3.3 Conclusions

In this chapter, the distance estimation scheme has been investigated using a rotational object in an indoor environment. The distance between the wall and the center of rotating object is measured. An AP and two STAs have been used. AP is placed on a blade. Two STAs are placed arbitrarily on a wall but not on same vertical line. The distance between the wall and the center of rotating object is measured with the intersection points of the circular surface of the two cones. Nowadays, with wireless communications scenarios, indoor collision avoidance applications between walls and flying drones can be initiated with this angle localization framework.

Chapter 4

RSSI based Distance Estimation in Different Environments

In this chapter, to estimate the distances between the wireless transmitter and receiver devices using the RSSI values, the curve fitting technique (CFT)-based approach [58] has been used. In this strategy, an access point (AP) transmits the RSSIs, and a station (STA) receives them. Due to the environmental catalyst factors (CFs) [75], the transmitted RSSIs become scattered, which produces uncertainty and may not produce a better outcome. Here, the mean RSSI-based approach is chosen, and with the standard deviations (SDs) [83], it is seen how much data are spread out among the mean ones. After a suitable path loss model (PLM) is chosen to estimate the distance using mean RSSIs. To make the PLM more accurate, the model is fitted to the consecutive actual distances and their corresponding mean RSSIs with the least-square technique to mitigate the errors significantly. Moreover, the estimated errors are calculated to the respective distances. Experiments have been conducted in three different regions, i.e., indoor, outdoor, and corridor with two Node MCU (ESP8266) modules [99], one as AP and another as STA.

4.1 System Model

Consider a distance finding scenario between two wireless devices using the RSSI values. Their distance is inversely proportional to RSSI, which monotonically decreases when the distance is increased. The signal strength represents the current state of the signal in excellent to poor conditions. However, the RSSI values of the AP to the STA are repeatedly changed at any distance due to the presence of environmental CFs. Since in different environments, the CFs are different. Therefore, RSSI readings will vary for individual atmospheres. Even the CFs are changed with the dynamic environments from time to time. So the short-time RSSI readings may not always produce better accuracies. In these circumstances, the statistical methods can play a significant role by providing a hypothetical conclusion, which not only reduces the methodology but also increases credibility. Therefore, to develop a distance estimation system using RSSI values, it is required to pick up reliable RSSI for a particular distance to get higher accuracy. Besides, in long distances, the CFs' influences on RSSIs are very strong. In most common wireless devices, isotropic antennas are used, which are built with omnidirectional signal radiation capabilities. For the omnidirectional signal propagation, the same amount of RSSIs can be observed in every direction, which monotonically decreases with an increasing circular perimeter around the AP. Therefore, the measurement RSSIs from the AP to any direction through a straight line represents the same signal condition in every straight direction. In this work, we focus on measuring the short-range-based Wi-Fi module's sensing capability, where the mean and SD-based approach has been taken into consideration. The distance estimation strategy using AP and STA can be seen in Fig. 4.1.

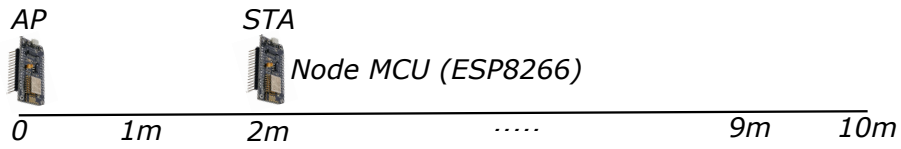

Figure 4.1: Distance estimation strategy in a straight line between AP and STA.

The mean RSSI value at any distance represents the average condition of a set of RSSI values, where the SD shows the RSSIs deviation of the set about the mean one. A high SD means the RSSIs values are very scattered around the mean. On the other hand, a small SD shows that RSSIs are very close to the mean. The formula for calculating the SD can be expressed by

$$s = \sqrt{\frac{1}{N-1}\sum_{i=1}^{N}(R_e^i - \overline{R_e})^2} \tag{4.1}$$

where R_e^i is the ith RSSI value, $\bar{R}_e$ is the mean RSSI value and N is the number of samples. Using this strategy, the RSSI trend to a distance for a certain time can easily be identified. With this RSSI trend, to get a more accurate distance, in this work, a proposed attenuation model (PESM) is generated, whereas, in the path loss model (PLM), the CFT is used to mitigate the errors in the extreme level such that its suitable parameters can be generated. Moreover, to verify the capability of this model, it is compared with the other models for existing parameters. Commonly this proposed model is used in the literature with the pre-selected parameters. However, in this work, the parameters are generated by the CFT. Due to the use of CFT, this model reaches higher accuracy by generating more appropriate parameters. The PESM can be written as

$$d_{PESM} = d_0 \times 10^{\frac{(R_0 - R_e^i)}{10\gamma}} \tag{4.2}$$

where R_0 is the initial RSSI value, R_e^i is ith the measured RSSI value, d_0 is the initial distance, and γ is the path loss exponent (PLE). First, we plot the actual model (ACTM) with the actual data. Then we compared it with the PESM; existing signal intensity attenuation model (SIAM), and free space propagation model (FSPM) [79] in different environments to find the best model. In the SIAM, the same PLM is used, but the pre-existing parameters are taken into consideration. Thus this may not sufficiently meet the CFT criteria. The FSPM with a large number of parameters can be expressed by

$$d_{FSPM} = \sqrt{\frac{P_t G_t G_r \lambda^2}{(4\pi)^2 P_r}} \tag{4.3}$$

where P_t and P_r are the transmitted and received powers, respectively, G_t and G_r are the transmitter and receiver antenna gains, λ is the signal wavelength. For isotropic signal propagation, G_t, G_r can be considered as 1, and the received power is measured by the equation $P_r = 10^{\frac{R_e^i}{10}}$. In an estimated model, the accuracy is a significant component of expressing its robustness. In this regard, the percentage can forecast this result more acceptably by increasing the chance of the comparison. To measure the error percentages in the estimated distance, the formula can be defined as

$$Error(\%) = \frac{(d_{actual} - d_{estimated})}{d_{actual}} \times 100 \tag{4.4}$$

where d_{actual} is the actual distance and $d_{estimated}$ is the estimated distance.

4.2 Measurement Background

To collect data in different environments, the same setup is used where we draw the mark at the respective positions from 0 m to 10 m in a straight can be seen in Fig. 4.1. The AP is always kept at the initial position of 0 m, and the distance of STA is increased one by one from 1 m to 10 m. Moreover, to these distances, the RSSIs are received by STA. It is observed that when the distance between AP and STA is close to each other, the received RSSIs are strong, and when the distances are monotonically increased, the RSSIs are decreased. Here, the distance is estimated using the mean RSSI value. To estimate the distance using a model, we calculate sample SD (4.1), mean RSSI, and received power (P_r) for the successive actual distances in the outdoor, corridor, and indoor, respectively can be seen in TABLE 4.1, TABLE 4.2 and TABLE 4.3. In this work, we consider the mean RSSI and their SD based approach to see their combined outcomes.

To each distance, a total of 300 RSSI values are taken. It can be seen from these

Table 4.1: Calculated outcomes in outdoor

Actual distance (d_{act} (m))	Sample SD (s (dB))	Mean (average) ($\bar{R}_e$ (dBm))	Received power (mW) (P_r)
1	1.7201	-71.2724	0.0000000746036
2	1.4928	-73.5946	0.0000000437058
3	2.3209	-74.4352	0.0000000360147
4	2.5681	-81.1328	0.0000000077040
5	1.9553	-80.9966	0.0000000079495
6	1.7268	-81.0897	0.0000000077809
7	1.8667	-87.1096	0.0000000019455
8	2.1177	-81.8637	0.0000000065107
9	2.0998	-84.6677	0.0000000034137
10	1.5578	-88.0564	0.0000000015644

tables that the SDs are high to some distance of more than 2 dB, which indicates that RSSI data are highly scattered, but this is inconsistent, i.e., they do not follow a particular pattern according to monotonic distances. This may happen due to the presence of high levels of CFs in the environment at a particular time. In the same way, we can see that the mean RSSIs do not also appear in any order for the respective distances. Moreover, in these tables, the received power is generated by the mean RSSI values. The received power is calculated to use in the FSPM.

Table 4.2: Calculated outcomes in corridor

Actual distance (d_{act} (m))	Sample SD (s (dB))	Mean (average) ($\bar{R_e}$ (dBm))	Received power (mW) (P_r)
1	2.3658	-68.1262	0.0000001539501
2	2.6989	-73.5049	0.0000000446179
3	3.9401	-81.8637	0.0000000065107
4	2.7636	-79.3588	0.0000000115909
5	2.5540	-83.1528	0.0000000048386
6	2.2814	-83.5747	0.0000000043906
7	1.9820	-84.7209	0.0000000033721
8	1.8456	-86.1295	0.0000000024380
9	1.8790	-86.5813	0.0000000021972
10	1.9507	-86.1860	0.0000000024065

4.3 Performance Evaluation

These experiments have been conducted inside the Jadavpur University on the rooftop of a two-storied building for the outdoor, a one-side open roof porch on the first floor of the same building for the corridor, and an all-side closed hall on the first floor of this building for indoor by placing the Node MCU (ESP8266), i.e., AP and STA on the floor. These measurements are done only considering the line of sight (LoS) static scenarios where human movement through these signals between AP and STA has not been considered. AP was connected to a power bank, and the station was connected to a laptop for storing the received RSSI values in computer files. The NodeMCU (ESP8266) operates on 2.4 GHz frequency bands of IEEE 802.11b/g/n standard. During these three experiments,

Table 4.3: Calculated outcomes in indoor

Actual distance (d_{act} (m))	Sample SD (s (dB))	Mean (average) ($\bar{R}_e$ (dBm))	Received power (mW) (P_r)
1	1.2043	-65.0531	0.0000003123848
2	2.7445	-80.1196	0.0000000097283
3	2.1855	-79.0598	0.0000000124170
4	2.2481	-81.7076	0.0000000067490
5	2.2035	-81.7973	0.0000000066110
6	1.7243	-82.5647	0.0000000055402
7	1.4646	-80.6112	0.0000000086872
8	2.0835	-86.2491	0.0000000023718
9	1.5592	-80.0465	0.0000000098935
10	1.6881	-88.1528	0.0000000015301

various electronic and Wi-Fi devices were activated in the surrounding buildings but using the service set identifier (SSID) of AP, the STA receives only particular RSSIs.

4.3.1 Results and Discussion

To evaluate the performance of the PESM, it is compared with the SIAM and FSPM. The comparative results of PESM, SIAM and FSPM can be seen in TABLE 4.4, TABLE 4.5, TABLE 4.6 for outdoor, corridor and indoor, respectively, where (d_{act}) is the actual distance and (d_{PESM}), (d_{SIAM}) and (d_{FSPM}) are the estimated distances by PESM, SIAM, FSPM, respectively. Moreover, their errors and error percentages are respectively, ($e_{PESM} = d_{act} - d_{PESM}$), ($e_{SIAM} =$

Table 4.4: Comparison table of outdoor

d_{act} (m)	$\bar{R}_e$ (dBm)	d_{PESM} (m)	d_{SIAM} (m)	d_{FSPM} (m)	e_{PESM} (m)	e_{SIAM} (m)	e_{FSPM} (m)	$e_{PESM}\%$	$e_{SIAM}\%$	$e_{FSPM}\%$
1	-71.27	1.0881	1	2.0479	0.0881	0	1.0479	8.81%	0%	104.79%
2	-73.59	1.4160	1.1430	2.6756	0.584	0.857	0.6756	29.2%	42.85%	33.78%
3	-74.43	1.5629	1.1997	2.9475	1.4371	1.8003	0.0525	47.9033%	60.01%	1.75%
4	-81.13	3.6973	1.7640	6.3729	0.3027	2.236	2.3729	7.5675%	55.9%	59.3225%
5	-80.99	3.6272	1.7503	6.2737	1.3728	3.2497	1.2737	27.456%	64.994%	25.474%
6	-81.08	3.6750	1.7597	6.3414	2.325	4.2403	0.3414	38.75%	70.6716%	5.69%
7	-87.10	9.6733	2.4885	12.6817	2.6733	4.5115	5.6817	38.19%	64.45%	81.1671%
8	-81.86	4.1038	1.8399	6.9324	3.8962	6.1601	1.0676	48.7025%	77.0012%	13.345%
9	-84.66	6.3043	2.1621	9.5738	2.6957	6.8379	0.5738	29.9522%	75.9766%	6.3755%
10	-88.05	11.6597	2.6278	14.1423	1.6597	7.3722	4.1423	16.597%	73.722%	41.423%

Table 4.5: Comparison table of corridor

d_{act} (m)	$\bar{R}_e$ (dBm)	d_{PESM} (m)	d_{SIAM} (m)	d_{FSPM} (m)	e_{PESM} (m)	e_{SIAM} (m)	e_{FSPM} (m)	e_{PESM}%	e_{SIAM}%	e_{FSPM}%
1	-68.12	0.7782	1	1.4256	0.2218	0	0.4256	22.18%	0%	42.56%
2	-73.50	1.4013	1.3629	2.6481	0.5987	0.6371	0.6481	29.935%	31.855%	32.405%
3	-81.86	4.1038	2.2051	6.9324	1.1038	0.7949	3.9324	36.7933%	26.4966%	131.08%
4	-79.35	2.8993	1.9090	5.1956	2.1007	2.091	1.1956	52.5175%	52.275%	29.89%
5	-83.15	4.9675	2.3750	8.0415	0.0325	2.625	3.0415	0.65%	52.5%	60.83%
6	-83.57	5.2996	2.4334	8.4418	0.7004	3.5666	2.4418	11.6733%	59.4433%	40.6966%
7	-84.72	6.3593	2.5994	9.6326	0.6407	4.4006	2.6326	9.1528%	6.2865%	37.6085%
8	-86.12	8.0817	2.8189	11.3285	0.0817	5.1811	3.3285	1.0212%	64.7637%	41.6062%
9	-86.58	8.7666	2.8932	11.9334	0.2334	6.1068	2.9334	2.5933%	67.8533%	32.5933%
10	-86.18	8.1633	2.8281	11.4025	1.8367	7.1719	1.4025	18.367%	71.719%	14.025%

Table 4.6: Comparison table of indoor

d_{act} (m)	$\bar{R}_e$ (dBm)	d_{PESM} (m)	d_{SIAM} (m)	d_{FSPM} (m)	e_{PESM} (m)	e_{SIAM} (m)	e_{FSPM} (m)	$e_{PESM}\%$	$e_{SIAM}\%$	$e_{FSPM}\%$
1	-65.05	0.5759	1	1.0008	0.4241	0	0.0008	42.41%	0%	0.08%
2	-80.11	3.2128	2.3805	5.6712	1.2128	0.3805	3.6712	60.64%	19.025%	183.56%
3	-79.05	2.7863	2.2396	5.0198	0.2137	0.7604	2.0198	7.1233%	25.3466%	67.3266%
4	-81.70	4.0125	2.6083	6.8089	0.0125	1.3917	2.8089	6.25%	34.7925%	70.2225%
5	-81.79	4.0647	2.6218	6.8796	0.9353	2.3782	1.8796	18.706%	47.564%	37.592%
6	-82.56	4.5475	2.7402	7.5151	1.4525	3.2598	1.5151	24.2083%	54.33%	25.2516%
7	-80.61	3.4375	2.4488	6.0015	3.5625	4.5512	0.9985	50.8928%	65.0171%	14.2642%
8	-86.24	8.2557	3.3877	11.4856	0.2557	4.6123	3.4856	3.1962%	57.6537%	43.57%
9	-80.04	3.1809	2.3705	5.6237	5.8191	6.6295	3.3763	64.6566%	73.6611%	37.5144%
10	-88.15	11.8937	3.7800	14.3001	1.8937	6.22	4.3001	18.937%	62.2%	43.001%

Table 4.7: Comparison of total and average errors (%)

Measured in respectively	Total error PESM	Total error SIAM	Total error FSPM	Average error PESM	Average error SIAM	Average error FSPM
Outdoor	293.12%	585.57%	373.11%	29.31%	58.55%	37.31%
Corridor	184.88%	433.19%	463.29%	18.18%	43.31%	46.32%
Indoor	297.02%	439.59%	522.38%	29.70%	43.95%	52.23%

$d_{act} - d_{SIAM}$), and ($d_{FSPM} = d_{act} - d_{FSPM}$) and ($e_{PESM}\% = \frac{e_{PESM}}{d_{act}} \times 100$), ($e_{SIAM}\% = \frac{e_{SIAM}}{d_{act}} \times 100$), ($e_{FSPM}\% = \frac{e_{FSPM}}{d_{act}} \times 100$) for the $\bar{R}_e$. From these results, it is observed that a high percentage of error occurs for PESM in the outdoor, corridor, and indoor, respectively 48.7025%, 52.275%, and 64.6566%. On the other hand, for SIAM and FSPM, these errors are respectively 77.0012%, 71.719%, 73.6611%, and 104.79%, 131.405%, 183.56%. These results show that the error percentages of PESM are comparatively less in different environments, but the errors of the other two models are relatively high. However, for some distances, PESM errors are very high for both environments. To generate the PESM, a pre-tested indoor datum is used, and with the CFT, its parameters are created. The created parameters are R_0=-69.324 dBm, d_0=1 m and $\gamma = 0.6852$. Then with these parameters, the estimated model is compared with the actual measured outdoor, corridor, and indoor datum. The initial mean RSSIs are the following, $\bar{R}_0$=-71.2724 for outdoor; $\bar{R}_0$=-68.1262 for corridor; $\bar{R}_0$=-65.0531 for indoor for the distance d_0=1 m, where for the SIAM, the $\gamma = 4$ is chosen. Moreover, for FSPM, $P_t = VI$ (power = volt $\times$ current), P_t is taken 0.00316227766 mW, P_r is taken from TABLE 4.1−4.3, where $G_t = G_r = 1$, as the antenna is isotropic and the wavelength is $\lambda = 0.125$ m as channel frequency is 2.4 GHz.

After the calculation of error percentages, with them, at first, total error percentages are calculated for the respective distances, then its average is calculated for different models in the outdoor, corridor, and indoor, respectively, which can be seen in TABLE 4.7. It can be seen that the highest average error percentage of

Table 4.8: Comparison for different environments

Actual distance (m)	Out Max (dBm)	Out Min (dBm)	Out Dif (dB)	Cor Max (dBm)	Cor Min (dBm)	Cor Dif (dB)	Ind Max (dBm)	Ind Min (dBm)	Ind Dif (dB)
1	-67	-75	8	-63	-77	14	-61	-68	7
2	-70	-80	10	-66	-85	19	-73	-87	14
3	-70	-86	16	-72	-89	17	-73	-87	14
4	-75	-88	13	-72	-89	17	-75	-90	15
5	-76	-90	14	-77	-90	13	-77	-89	12
6	-77	-88	11	-78	-89	11	-74	-88	14
7	-82	-93	11	-78	-89	11	-76	-85	9
8	-77	-91	14	-79	-92	13	-80	-91	11
9	-80	-90	10	-81	-92	11	-77	-88	11
10	-82	-92	10	-81	-91	10	-83	-93	10

PESM is 29.70%, and its least one is 18.18%. On the other hand, the highest and lowest percentages of average errors of SIAM and FSPM are 58.55%, 52.23%, and 43.31%, 37.31%, respectively. The comparison shows that the PESM achieves average error percentages under the SIAM and FSPM at both times. Even the highest average error percentage of PESM is less than the least ones of SIAM and FSPM. With these outcomes, one can say the PESM is much better than others for any application scenario.

Combining these three environmental errors, the average of average error percentage (i.e., an average of outdoor(O), corridor(C), and indoor(I) together) has been calculated. For PESM the total of average error percentage is $(d_O + d_C + d_I)$ = 77.20321% and average of average error percentage is $(d_O + d_C + d_I)/3$ = 25.7344%; for SIAM the total of average error percentage is $(d_O + d_C + d_I)$ = 145.83578% and average of average error percentage is $(d_O + d_C + d_I)/3 = 48.61\%$

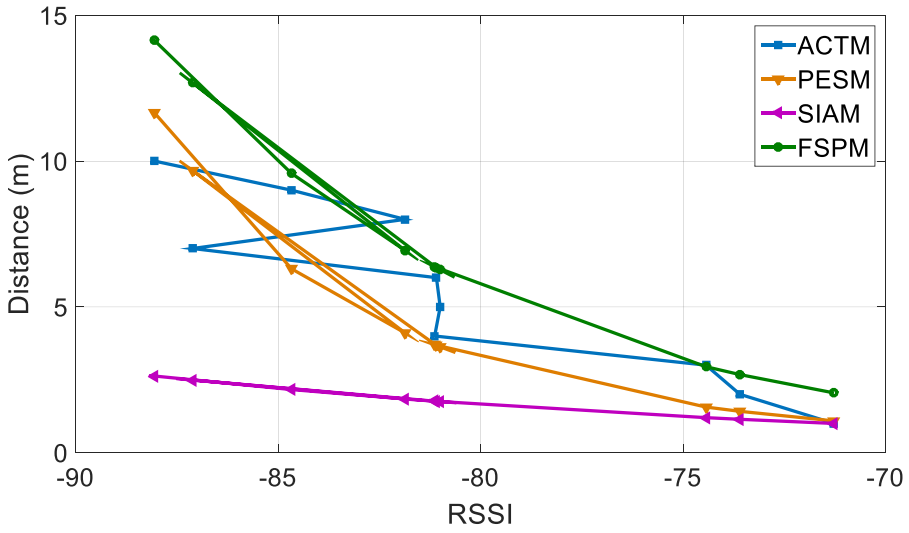

Figure 4.2: Comparison among PESM, SIAM and FSPM for outdoor.

; for FSPM the total of average error percentage is $(d_O + d_C + d_I) = 135.87937\%$ and average of average error percentage is $(d_O + d_C + d_I)/3 = 45.2931\%$. From these outcomes, it is observed that, again, the average of average error percentage of the PESM is very low compared to other models. On the other hand, SIAM has a higher average of average error percentage than FSPM. The above results show that the PESM outperforms the SIAM and FSPM when CFT-based parameters are used for this model.

From these figures (drawn from TABLE 4.4-4.6), Fig. 4.2, Fig. 4.3 and Fig. 4.4, it can be said that ACTM is more likely to PESM than SIAM and FSPM. Besides, from these three figures, it is observed that every time the FSPM graph goes above the PESM. On the other hand, the SIAM graph goes below the PESM. Therefore errors are huge for them. As well as, the parametric process of PESM is so simple and can be easily adapted for any type of data. Since the RSSI and distance are highly dependent, therefore, PESM is the more suitable option to represent these data. In contrast, the parametric process of SIAM and FSPM is not proper with the data. Even these models are highly affected by their parametric constraints. Also, we have calculated the maximum (Max) and minimum (Min) of 300 RSSIs, and their difference (Dif) for each distance for outdoor (Out), corridor (Cor), and

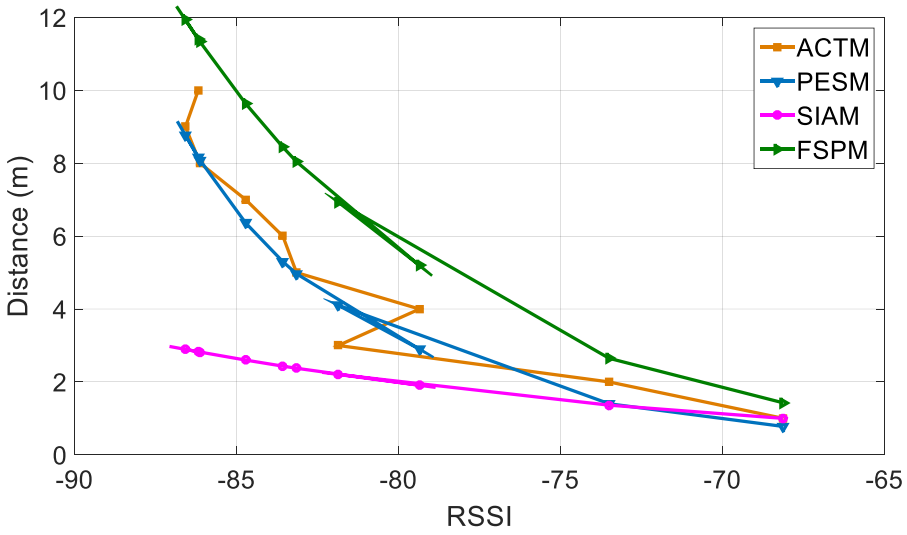

Figure 4.3: Comparison among PESM, SIAM and FSPM for corridor.

indoor (Ind) can be seen in TABLE 4.8. The maximum difference is seen at 19 at 2 m in the corridor, which means that strong RSSIs sometimes can be affected larger by the environment.

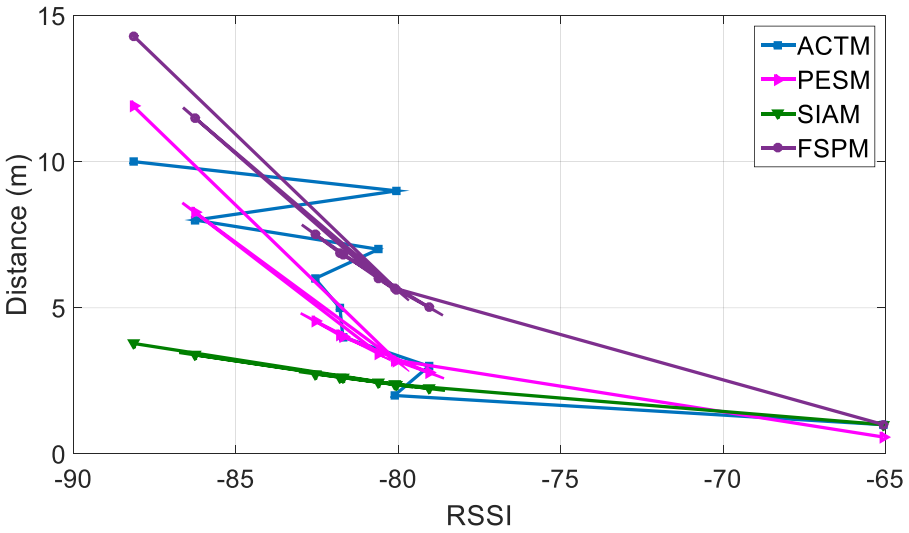

Figure 4.4: Comparison among PESM, SIAM and FSPM for indoor.

4.4 Conclusions

The Node MCU (ESP8266) is a low-cost module and is easily available in the online market. This device is not only used in various wireless network applications but also has several uses in the internet of things (IoT) communications. Since the current wireless architecture is moving toward IoT-based solutions, thus MCU (ESP8266) has the possibility to meet the current requirement to provide better performance with a low budget. Therefore, to estimate the distance using RSSI values, this module is taken into consideration. Moreover, with this module, a proper distance measurement procedure has been developed. First, RSSIs are measured to the respective distances through a straight line. Then a proper PLM is chosen, and in this model, CFT is used to find a higher accuracy. It is observed that the PESM provides better accuracy than some other models of pre-selected parameters. Even when the measurements are largely affected by the environment, the proposed model is highly efficient considering different points of view. The comparison also shows that the CFT is more reliable than the model of selected parameters. The RSSI-based distance estimation has an essential requirement for smart infrastructure to determine the stability of the

communication.

Chapter 5

RSSI-Fingerprinting-based Smartphone Localization System for Indoor Environments

In this chapter, an RSSI-fingerprinting-based positioning scheme has been investigated, considering indoor environmental changes. The positioning skill has been studied utilizing at most three APs' distances, whereas using three APs' RSSI conditions, the indoor positions of a smartphone are localized. To choose a proper RSSI value for accurate positioning, some special RSSI values-based approaches, i.e., mode and mean, are taken into account to find the better one to achieve the most outstanding accuracies. In each experimental room, the smartphone collects the RSSIs from multiple APs together using a Wi-Fi analyzer application (APP) [30] at different points to locate its position. The random position is localized inside based on 3 noisy RSSI values from 3 APs. It is considered that the environment does not changed for a fixed time frame. A training technique is provided to get distance from RSSI values. This technique considers the fixed environmental parameters. For training, $m \times n$ reference points are used. After, for each distance, an average is calculated with the K-nearest-neighbor (KNN)

of the special RSSI value. Then a suitable signal intensity attenuation model (SIAM) is chosen to establish the relationship between RSSIs and distances. For establishing this relationship, the nonlinear regression analysis technique (RAT) [35] is used.

5.1 Overview

In modern communication technologies, wireless fidelity (Wi-Fi) has achieved dramatic interest due to extensive adoption and widespread deployment. The Wi-Fi positioning techniques with the RSSI have grown mainstream, including the benefits of economical cost, extensive coverage, and does not need any additional hardware, which has vast regular applications in sensing, monitoring, and communications [91]. However, researchers face several challenges in developing a real-time kinematic RSSI measurement system due to the changing surrounding environments from time to time [10]. It is seen from the current literature that most of the positioning approaches suffer from the lack of proper selection of RSSI values, which cannot reduce the errors significantly. In some cases, it creates a huge impact on the desired performance. Because in the signal propagation, with the ranges of technologies, the selection of RSSI (e.g., mode or mean, etc.) is the principal reason for various kinds of positioning errors [64]. The motivation behind accepting the mode and mean RSSIs are as follows: (a) The mode RSSI value [89] regularly appears in a particular position even when the environmental noises affect the measurements. Therefore considering traditional environmental conditions, its position determination capability is quite reliable and straightforward. (b) The occurrence of mean RSSI depends on the whole sample observed during the measurements. Thus, its reliability is a bit unstable because if a high fluctuation is seen in the RSSI data to some positions, it may make the worst decisions. (c) The largest RSSI to any position shows the highest achievement of signal strength. Since the most common RSSIs are weaker than the largest one, it appears very rarely in this position. Thus it should be less considerable for precision achievement. (d) Similarly, since the most common RSSIs are stronger than the smallest one, it also less significant. (e) The median RSSI is the mod-

erate value in a list ordered from smallest to largest. It can often be changed to every position depending on the volatile environments that can highly influence the accuracies. Further, the ranges of wireless devices (with the same technology) are different such as multiple Wi-Fi routers with diverse configurations have different communication ranges. Hence, numerous data characters prediction with various types of devices is typically very hard, which can not explain current issues adequately. In radio wave technologies, the RSSI is considered a dominant ranging method because it determines sensors' locations without employing special hardware, which reduces cost as well as energy consumption. However, due to omnidirectional signal radiation, position localization using a single Wi-Fi AP will be very difficult. Also, it may not produce desired results regarding the signals' uncertainties [28]. The same configured APs have been used for experimental reviews, where different reference points are drawn by imagining a grid on the floor in experiment rooms. The position of each reference point is inside every cell of the grid. Two indoor atmospheres have been considered for judging the interpretation with different scenarios but the same dimensions. One is an auditorium hall, and another is a computer lab. The first one is full of wooden sofas, and the second one is full of wooden furniture as well as electronic devices. These two scenarios are considered to observe the change of RSSIs in varied situations. Moreover, in each part, at most, three nearest APs' RSSIs are used. For this, to the monotonically increasing reference points distances from different APs', proper special RSSIs are selected. Due to the high dependency between RSSIs and their distances, their correlation cannot express by a linear shape. Thus the nonlinear model is a compelling option as it presents more flexibility than a wide variety of linear models because it is based on a least-square iterative procedure [50]. That modifies its measuring parameters significantly and re-evaluates them until it obtains the best fit. This procedure is so satisfying because it can describe data characteristics within a moment. The KNN strategy [17], and RAT make the SIAM more skillful in producing higher precisions for distance measurements. Lastly, the smartphone's positions are estimated at different random points (RPs) using three APs positions and distances. In this technique, simultaneously, three APs RSSIs are projected together through differ-

ent rows or columns of RPs. Moreover, their RSSIs at different RPs are different. Therefore, considering the RSSI states concurrently utilizing different APs' distances, the RP positions can smoothly be measured where Euclidian geometry [37] may be required. For performance analysis, experiments and simulations have been conducted with various classes of data considering different scenarios. The comparative results exhibit that with the mode RSSI values, the proposed algorithm produces the errors under the mean RSSIs as well as existing algorithms present in the literature for both experimental rooms, which confirms the proposed algorithm is more accurate, simple, effective, reliable, and robust than other approaches.

5.2 System Overview

5.2.1 Categories Of Fingerprints

Among all range-free localization methods, the most popular one is RSSI fingerprinting because of its high accuracy compared to others. This technique does not need line of sight (LoS) measurements, thus achieving high applicability in complex environments. It is also familiar as the pattern matching-based system. Which can be categorized into two kinds, including offline and online fingerprints [13]. In the offline type, a large number of RSSI values from available APs are collected for certain times to different positions inside their coverage zones. In particular, a grid spacing area of one meter is more suitable. However, this empirical grid may vary according to many situations. Obviously, more parameters by pre-signal observation provide unique fingerprinting to present better localization accuracies. Moreover, there are no predefined constraints on time durations to provide optimized RSSI fingerprint outcomes. Consequently, the identity (ID) of an AP and its corresponding RSSI values are recorded as columns in a database. Different rows of the database contain the RSSIs of different APs for the RPs. This database basically reflects the special distribution of RSSIs to a point considering different APs' distances. On the other hand, in the online type, a device

of unknown position reports its measurement by the RSSI samples for beacon APs, which is analyzed by the data investigating server. After, the server runs the existing fingerprint algorithm to compute the location associated with the reported RSSI measurement. Finally, the estimated location sends back to the particular device.

5.2.2 Fingerprinting Mechanism

Consider a room of dimensions $l \times w \times h$, where l stands for length, w stands for width, and h stands for height. It assumes that the floor area $l \times w$ is discretized into a set of known positions, where $\theta_i = [x_i, y_i]$, $i = 1, 2, \ldots, z$ represents the 2-dimensional (2-D) Cartesian coordinate of these positions with parameter i. In every position, there has a wireless transmitter device that preserves its unique ID. Within the $l \times w$ region, $m \times n$ (m rows and n columns) reference points are drawn inside the grid cells with equal intervals. To these reference points s with coordinate $\phi_j = [x_j, y_j]$, $j = 1, 2, \ldots, g$, the RSSI values are collected from each position ϕ_i together. Consequently, RSSIs are scanned for a certain period of time to record many temporal samples to tolerate some degree of noise. For the unique ID, k temporal samples are collected in each reference point. Then suitable APs are chosen on the basis of the strongest RSSIs for reference points locations estimation.

5.2.3 Sample Classification Procedure

The APs are kept in the known positions $\theta_i = [x_i, y_i]$, $i = 1, 2, \ldots, z$ which radiate the omnidirectional signals. For smartphone (S) localization, their RSSIs are collected in different reference points, and then the data is forwarded to the server for the following actions. Where the original positions are calculated by Euclidian geometry. In each reference point $\phi_j = [x_j, y_j]$, $j = 1, 2, \ldots, g$; s RSSI samples are collected from every AP.

From AP_i, get $RSSI_i = \{rssi_1, rssi_2, \ldots, rssi_s\}$,

- $rssi_m \leftarrow Mode(RSSI_i)$,
- $RSSI_i^u = \{rssi_p | rssi_p > rssi_m\}$,
- $RSSI_i^l = \{rssi_q | rssi_q < rssi_m\}$,
- These are two classes $RSSI_i^u$ & $RSSI_i^l$ and a value $rssi_m$,
- Using k-nearest neighbourhood (KNN) classify $rssi_m$ either in $RSSI_i^u$ or in $RSSI_i^l$,
- Resultant $rssi$ = average of the set in which $rssi_m$ is in.

5.2.4 Algorithmic Description

The RSSI-based fingerprint positioning algorithm is one kind of evolutionary computation complement to traditional laborious and expensive techniques, which can be operated by installing some simple wireless devices easily available in the markets. The proposed system can freely be adapted for any type of infrastructure to tackle the requirements of various positioning applications [54]. However, due to environmental uncertainties regarding the presence of dynamic catalyst factors (CFs), it is hard to achieve higher precision in position estimation [55] considering various constraints. Therefore, to mitigate the fingerprint positioning error significantly, an improved algorithm is required to overcome such CFs' impacts on wireless signals. So in this paper, a new technique has been presented. Our positioning scheme is drawn in algorithm 5.1.

Each reference point belongs inside the intersecting coverage of multiple APs, where the grid is considered to partition the sensing area into multiple segments. Every segment is thought of as a grid cell, and every reference point belongs to a cell. Besides for having an isotropic antenna, AP radiates the omnidirectional signal.

Algorithm 5.1 Proposed Positioning Scheme

Require: Measured RSSI value $RSSI_m$;

Ensure: Estimated location P_j;

1: Initialize the indoor atmosphere;
2: Plant APs in known positions;
3: Plot reference points inside the cells of the grid for RSSI fingerprint positioning;
4: Create a database using APs' IDs and RSSIs for respective reference points;
5: Organize the RSSIs dataset for each AP to the reference points with monotonically increasing distances;
6: **for** $\theta_i : i = 1$ to z **do**
7: **for** θ_j: $j = 1$ to g **do**
8: Create a special RSSI value (e.g., mode or mean) by them;
9: Determine the KNN values of the special RSSI;
10: Calculate an average with the KNN RSSIs;
11: Ignore accepting the same and similar average KNN RSSIs from any of these two APs;
12: Collect the monotonically decreasing average KNN RSSIs corresponding to the gradually increasing RP distances;
13: **end for**
14: **end for**
15: Define a proper SIAM to estimate the distances between APs and RPs using average KNN RSSIs;
16: Use RAT to SIAM such that error can be mitigated significantly;
17: Estimate distances with SIAM for the corresponding average KNN RSSIs;
18: Estimate the location of each RP (P_j) considering the distances from the APs;

5.2.4.1 Time Complexity

For this algorithm, statements one to five and fifteen-eighteen each run once. Moreover, inside the loops, statements eight to twelve each run g number of times. Therefore time complexity of this algorithm can be written as

$$T(n) = \mathcal{O}(9 + z(6g)) \tag{5.1}$$

where z is the array length of the first loop and $n = zg$ is any variable.

5.2.5 Existing Attenuation Models

To estimate the distance between transmitter and receiver using RSSI, transmission loss is a major factor due to several environmental issues affecting proximity and channel conditions. For the special resolution of the measuring rule of such an uncertain signal, the monotonic relation between RSSI and distances should be established by a suitable attenuation model. Many research works are present in the literature to determine the relationship between RSSIs and distances by defining various formulas. However, due to different parametric constraints, all these models cannot provide reasonable proximity considering ever-changing dynamic environments. Along with the properties of some attenuation models, their pros and cons have been discussed in the following.

5.2.5.1 Path loss model (PLM):

Among all attenuation models, the PLM [12] is most commonly utilized in the literature using a different shape. However, the general form of the PLM can be described by,

$$d = d_0 \times 10^{\frac{(RSSI_0 - RSSI_m)}{10\gamma}} \tag{5.2}$$

where $RSSI_0$ and $RSSI_m$ are the received RSSI values to the positions which

have the distances d_0 and d from the transmitter, respectively, and γ is the PLE. The d_0, $RSSI_0$, and γ are known in advance through modeling. Thus, the unknown distance d is calculated by the measured $RSSI_m$. Although in the free space, γ is recognized as 2, with the modeling, less PLE than 2 can be achieved. The PLE depends on environmental CFs. If the CFs increase naturally, the PLE increases, and if the CFs decrease, the PLE decreases. Therefore, any little variation in PLE can change the measured error significantly. Besides, representing the fluctuating character of RSSI data with pre-selected parameters may lead to huge errors. However, those challenges can be overcome by utilizing the RAT-based procedure. Since the RSSIs and distances are highly dependent on each other and form a nonlinear shape. So, RAT based least square technique with PLM can easily express their relationship at a glance using a curve-fitting tool because it generates a nonlinear exponential paradigm.

5.2.5.2 Free-space propagation model (FPM):

This attenuation model is commonly known as the Friis transmission equation [9]. Further, this formula also can be expressed in a different shape, but its general form is presented by

$$d = \sqrt{\frac{P_t G_t G_r \lambda^2}{(4\pi)^2 P_r}} \tag{5.3}$$

where P_t and P_r are the transmitting and receiving powers, respectively, G_t and G_r are the transmitter and receiver antenna gains, λ is the signal wavelength with the channel frequency f. For isotropic signal propagation, $G_t = G_r$ can be considered 1, and the received power is measured by the equation $P_r = 10^{\frac{RSSI_m}{10}}$. With these parameters, the distance d between two devices is calculated by the measured $RSSI_m$. One can observe that the formula contains a large number of parameters, which are bounded by several constraints. Because of different kinds of constraints in different parameters, this formula is extremely affected to provide higher precision, which may not be sufficient to express any suitable

nonlinear expression even when RAT is used.

5.2.5.3 Polynomial regression model (PRM):

When a simple linear regression model fails to express the relationship between independent and dependent data or is not capable of drawing the best fit model. In such conditions, the PRM [48] can be used to overcome this problem by establishing a curvilinear relationship. The PRM can be represented by

$$d = a_n \times RSSI_m^n + a_{n-1} \times RSSI_m^{n-1} + \ldots + a_1 \times RSSI_m + a_0 \tag{5.4}$$

where a_i $(i = 0, 1, 2, \ldots, n)$ are the coefficients, $RSSI_m$ is the measured RSSI variable, and n is the exponent. Although PRM support for generating a proper nonlinear shape to express the correlation between different variables, its restriction in coefficients does not allow it to represent all kinds of data efficiently. Therefore, RAT-based PRM may not provide the desired results in every situation considering the monotonic shapes of variables.

Among these three models, it is seen that the PLM is highly efficient because the model is nonlinear and monotonically changes with an exponential progression. Thus, in this work, PLM has been used as SIAM to obtain better precision.

5.2.6 Data Filtering Methods

In any localization system, various techniques are used to generate proper data so that estimated errors can be reduced significantly. Among all existing data selection techniques, the most commonly applied strategies are KNN, KF, and random forest (RF). However, in real-life applications, every technique has significant drawbacks. In the following, the principle of these methods and their weaknesses have been discussed.

The KNN method [92] is based on the selection of special outcomes. At first, a special value (e.g., mean or mode) is selected from a large field of measured

samples. Then some nearest values are chosen of this selected value, and the result produces by combining them. Consequently, this method entirely depends on the choice of the special sample and the nearest ones. The wrong choice of sample significantly influences the determined positions. Therefore data need to choose as close as possible.

The KF method [19] is used to decide state vectors based on linear dynamical approaches in a state-space layout. The method defines the progress of the present state, considering the situations of the earlier state. Together, the earlier state and control vector are included in the process noise vector then the present state is determined. After that, the measurement vector is calculated for evaluation. Therefore, the method is more time-consuming, as well as the non-linear data representation with this method, may lead to lower precision.

RF method [61] is used widely in classification and regression problems. It builds decision trees on different samples, and their majority votes are taken for classification, and the average is taken in case of regression. This method is based on ensemble learning, which creates a distinct subset from samples of data with replacement, and their final output is based on the majority. The main constraint of RF is that many decision trees can make the method too complicated and ineffective for real-time forecasting.

The above discussion suggests that RSSI-based position estimation with the KNN method is more efficient in delivering the most remarkable reliability than other traditional methods in ranging-based localization processes. So in this work, to effectively deal with current phenomena, a simple and robust KNN-based positioning approach has been investigated. Such that a higher precision can be achieved.

5.2.7 Environmental Impact

In wireless communications, the RSSI indicates the real-time channel intensity of the transmitting signal to the receiver device. The RSSI condition is inversely proportional to the distance, i.e., if the transmitter and the receiver devices are close

to each other indicates a strong RSSI, and the RSSI is monotonically decreased when their distance is gradually increased. Therefore, according to the RSSI intensity, the signal can be divided into different categories, such as excellent, good, fair, and poor. It is not only influenced by the distance but also affected by current environmental CFs. The CFs are changed when the environment is changed. Consequently, the RSSI also varied. Various CFs usually influence the RSSI-based information in the indoor environment, particularly noises, shadows, multipath, fading, human body, weather, temperature, metal components, electric devices, various radio signals, etc. They not only individually impact the wireless measurement but also may generate different types of combinations together. For instance, at a certain time, if we think that three CFs are present in the current environment, influencing the RSSI measurements, which are human body (H), reflection (R), and temperature (T). If we consider the signal as a particle, then the vector effects of $\vec{H}$, $\vec{R}$, and $\vec{T}$ on it are not only individuals but also the different combinations of their products, which is defined by the RSSI states. Thus the resultant impact will be the summation of various combinations of magnitudes of these three factors that can be expressed as

$$\begin{aligned} cf_3 = f(|\vec{H}|, |\vec{R}|, |\vec{T}|) = |\vec{H}|+|\vec{R}|+|\vec{T}|+(|\vec{H}|\cdot|\vec{R}|) + (|\vec{H}|\cdot|\vec{T}|) \\ +(|\vec{R}|\cdot|\vec{T}|) + (|\vec{H}|\cdot|\vec{R}|\cdot|\vec{T}|) \end{aligned} \tag{5.5}$$

Every environmental CF can decrease or increase according to the current circumstances. Consequently, this summation will be changed. It is unknown to us how much CFs are present in the current environment and how they affect the signal. The CFs in any environment may be infinite. Therefore, different algorithms are presented in the recent literature to overcome the influence of CFs for RSSI-based localization schemes to improve positioning accuracy.

5.2.8 Regression Technique

The regression strategy is the most common word in the statistical analysis, where the intensity and character of sample data are determined considering the dependent (distance) and independent (RSSI) variables applying an estimated model [87]. Where the estimated model is fitted to the particular variables to fetch the highest precision to establish their relationship. Besides, it can be employed to determine the characteristics of the associated variables at a glance. To this process, the nonlinear least-squares method produces a much bigger and more general class of ranging precisions. Unlike linear regression, there are fewer restrictions on the estimated model's parameters. Therefore, with the nonlinear regression strategy, any shape of ranging data can present more efficiently. Since the RSSI and their distances are highly correlated; thus only a nonlinear regression model is a compelling alternative to predict their conditions. Therefore this paper proposed a nonlinear regression scheme, where the proposed PLM is fitted to the data using the least-square technique to establish the relationship between RSSI and distance in a monotonic form. To increase the capability of PLM's parameters, different benchmarks are taken into account, including coefficient of determination (R^2), the sum of squared error (SSE), and root mean squared error (RMSE) . The R^2 evaluates how effectively a model is represented and predicted by the scattered data in different ranges. The R^2 more than 0.98 establishes that 98% of the modification in the character of distances represented by the RSSIs. The SSEs and RMSEs decide how the data associated with the model brings to the most desirable fit. The RMSE gives a comparably high significance than SSE for larger errors. The characteristics of PLM validate that the use of a regression technique is more beneficial. Because the shape of PLM is ubiquitous in natural phenomena, and its parametric systems are well understood. To estimate the position with PLM, the error between the actual and the estimated distance is minimized based on γ and $RSSI_0$. The estimated results depend explicitly on the attenuation model and implicitly on the environment. The environmental CFs influence both γ and $RSSI_0$. So a proper analysis is required to minimize the localization error to furnish a higher solution for balancing the environmental

matters and measurements.

5.2.9 Technological Comparison

In developing reliable WSNs, the main contribution goes to managing the system in its technology. Therefore to implement a WSN-based localization system [4], researchers mainly focus on the technological specifications. Therefore, in this literature, to properly judge technological ability, a comparative overview has been presented of similar technologies. Here the most popular technologies such as Wi-Fi, Bluetooth, and ZigBee are compared [8] because they are almost built with similar specifications as well as form a point to multi-point (P2MP) network topology. However, their operating capabilities are quite different, including the data rate, range, and sensitivity. The comparison of different technologies is shown in TABLE 5.1. In a typical comparison, it can be observed that Wi-Fi outperforms other relative technologies such as Bluetooth and ZigBee in the sense of range, data rate, and price. Further, Wi-Fi is widely used on a large scale of applications due to its outstanding features in modern communications systems. Besides, the smartphone supports Wi-Fi technology. On the other hand, if we compare different Wi-Fi standards, e.g., IEEE 802.11b/g/n, IEEE 802.11ax [25], IEEE 802.11ac, and IEEE 802.11n (5 GHz) [18]. It can be observed that the frequencies, data rates, and sensitivities are much higher, and the ranges are much lower for IEEE 802.11ax, IEEE 802.11ac, and IEEE 802.11n (5 GHz) than IEEE 802.11b/g/n, which can increase some degree of efficiencies and capacities. However, their costs are four to seventh times compared of the traditional one. That will influence the budget for installation.

5.3 Implementation Background

To evaluate the performance of the proposed RSSI based fingerprinting algorithm, experiments are conducted inside a departmental building using a network of IEEE 802.11b/g/n Wi-Fi protocols installed in two rooms, their walls built with various materials such as the combination of concrete and gypsum,

Table 5.1: Comparison between similar technologies

Technology	WiFi				Bluetooth	Zigbee
Standard	IEEE 802.11b/g/n	IEEE 802.11ax	IEEE 802.11ac	IEEE 802.11n	IEEE 802.15.1	IEEE 802.15.4
Frequency	2.4 GHz	5/6 GHz	5 GHz	5 GHz	2.4 GHz	2.4 GHz
Range	10-150 m	10-40 m	10-50 m	10-100 m	10-50 m	10-100 m
Data Rate	54 Mb/s	1.8 Gb/s	1.3 Gb/s	433 Mb/s	25 Mb/s	20-250 Kb/s
Network Topology	P2MP	P2MP	P2MP	P2MP	P2MP	P2MP
Spectrum	Unlicensed	Unlicensed	Unlicensed	Unlicensed	Unlicensed	Unlicensed
Sensitivity	-98 dBm	-79 dBm	-84 dBm	-92 dBm	-97 dBm	-100 dBm
Price	$ 10	$ 70	$ 50	$ 40	$ 10	$ 30

but have fiberglass doors and windows. Experimental scenarios of the auditorium hall and computer lab can be seen in figure 5.1 and figure 5.2, respectively. The computer lab fills with computers and electronic gadgets along with wooden furniture. On the other hand, most of the portion of the auditorium hall fills with wooden sofas. For the proposed WSNs, Wi-Fi supported APs are used for localization systems that have a typical omnidirectional coverage range of 32 m in indoor environments. Three Wi-Fi APs are planted in three different positions inside each room, i.e., at two corners and the center. Both APs radiate the omnidirectional signals together, covering the room. Moreover, using the developed Wi-Fi analyzer APP, a smartphone simultaneously records APs RSSI samples

from different reference point locations. Then it forwards these samples to the server, where the server analysis them using a software-defined strategy to choose better ones. A total of 30 RP positions are plotted on the floor of each room, considering 5 rows and 6 columns by maintaining equal intervals. Every cell of grid around each reference point have a dimension of 1.30 m × 0.98 m. Due to different environmental scenarios in each room, their CFs must be diverse. Besides, LoS, NLoS, and multipath signal radiations also affect the RSSI states. Consequently, two localization scenarios are considered in every room, i.e., static and dynamic. To conduct the experiments, both APs and the smartphone are kept at the height of 1 m installed on the tripods at the static condition. On the other hand, for the dynamic condition, APs are kept at the same height and same positions as static, but a person walks inside each cell of the grid by gripping the smartphone in hand. For each reference point, the smartphone collects a total of 50 RSSI samples from every AP. However, only those APs' RSSIs are taken for calculation, which have more strong RSSI outputs. Then from any AP's set of RSSIs, the desired part is chosen using the proposed decision tree method for each smartphone's location. From it, the mode or mean special RSSI value is calculated. Next, generally, its 5 nearest neighborhood (5NN) values are selected to calculate their average. To minimize the errors for distance estimation, RAT is used in the PLM. Finally, the smartphone's position in each reference point is measured using the APs' positions and the distances between APs and reference points, where this investigation has been conducted by recognizing the presence of surrounding outdoor radio devices. Even some other smartphones are taken into consideration where their users operate them from different indoor random positions during both static and dynamic experiments.

5.4 Performance Assessment

The effectiveness of the proposed scheme has been studied by designing a simple prototype. In the proposed system, each smartphone's position to the RP is localized with the help of RSSIs of APs. First, training data is collected from the reference points. Then, on the basis of the distances from the training data,

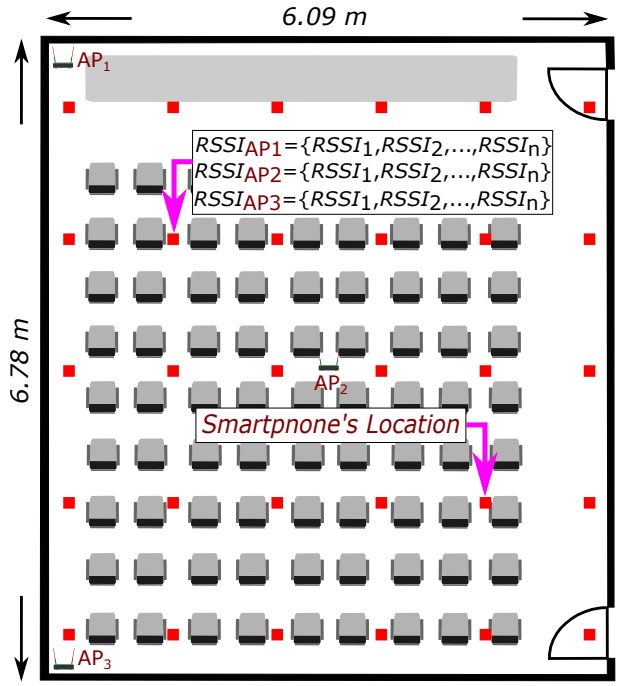

Figure 5.1: Experiment scenario for auditorium hall.

the test is performed to different RPs to calculate the errors. Where in both scenarios, the original distance between two positions has been calculated with the help of measuring ribbon and Euclidian geometry.

5.4.1 Results and Discussion

With the largest R^2 = 0.9988 and least SSE = 1.158 and RMSE = 0.226, the PLM establishes a better relationship between average KNN of mode RSSI values and distances. For utilizing the RAT to the proposed PLM, the parameters are generated for the auditorium hall $d_0 = 0.5674\ m$, $RSSI_0 = -42.34\ dBm$, and $\gamma = 0.7356$ by the modeling in Matlab [70]. Moreover, the error is considered based on this model in training environment.

The comparison between absolute errors considering the testing data of the average KNN of mode RSSIs for different rooms in static conditions can be seen in TABLE 5.2, where the symbols 'ah' stands for auditorium hall, and 'cl' stands

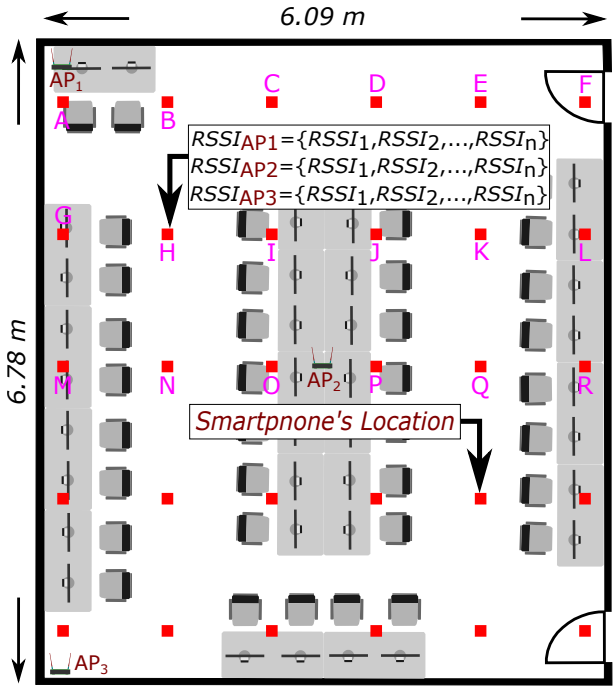

Figure 5.2: Experiment scenario for computer lab.

for the computer lab.

It is observed that for the initial original distance of 0.5674 m, the percentages of error for 'ah' and 'cl' are 39.32% and 56.64%, respectively, but at the original distance of 0.6038 m, the error percentages are increased and reached 63.13% and 74.66% respectively. Although the difference between these original distances is 0.0364 m, the percentages of error gain a high rise. The reason behind that is the original distance of 0.5674 m is measured from AP_2 (i.e., central AP), whereas the original distance of 0.6038 m is measured from AP_1 (i.e., corner AP). The original distance from nearest RP of AP_2 is less than the distance from nearest RP of AP_1. Since the position of AP_1 is in the corner, where the surrounding noises are very high than in other regions of the room because the signals from multiple APs are quickly reflected and refracted from the walls, which infect the RSSIs measurements by multipath radiations. Relatively the error effects on the central positions are shallow. However, in the intermediate distances (1.1349 m to 4.5396 m) for both rooms, the error percentages are relatively pettier

(41.00% to 51.29%). For the long distances (i.e., from 4.7348 m to 5.8318 m), the system achieves higher accuracies, where the error percentages are seen between 31.23% and 35.94% for 'ah' and 34.83% and 39.73% for 'cl'. This happens because when two APs' distances are extended for consecutive RPs, their signal strengths become very weak to these RP positions. Therefore, the signal of one cannot affect others significantly. So the error percentages level is minor. In contrast, when one AP's signal strength is stronger than others, noises become larger. So measurement states are quite unstable. Thus the errors of the intermediate distances are comparatively large.

After, the mode RSSI value is compared with the mean RSSI value for both the 'ah' and 'cl' in static situations applying the same average KNN data filtering approach to estimate distance. It can be observed from figure 5.3 that for mode RSSI values, the errors are shallow, and the error difference between these two rooms is not too big in static conditions. The highest error in the 'ah' and the 'cl' are seen at 1.8930 m and 2.0314 m, respectively, at the original distance of 5.8318 m. Their maximum error difference between 'ah' and 'cl' is 0.2188 in 5.6745 m. On the other hand, the errors for utilizing the mean RSSIs are very high compared to mode ones. The largest errors observed for the mean RSSIs in the 'ah' and 'cl' are 2.3924 m and 2.7512 m, respectively, at the original distance of 5.8318 m, where their large error difference is 0.4676 at 4.5396 m. From this figure, it also can be observed that the errors in the 'ah' are always under the 'cl' for both the mode and mean outcomes to every RP position. The errors increase in the 'cl' may be due to the presence of electronic devices, which have a larger impact on the RSSIs states due to signal diffractions. In addition, the CFs effects are changed from time to time to any position. Subsequently, the RSSI readings are changed. The comparison between the average KNN of mode and mean RSSI values in different environments in static states confirms that the mode RSSIs outperform the mean RSSIs with the proposed localization algorithm. Therefore, to validate the feasibility of the mode RSSI values, different data filtering methods have been compared with each other to verify their effectiveness for the proposed technique. In this case, to the proposed algorithm, the KNN-based data filtering process is replaced by KF [97] and RF [74] methods in static conditions where for the KNN

Table 5.2: Comparison of test results between two experimental rooms

Serial No.	Actual Distance (m)	Average $RSSI_{ah}$ (dBm)	Average $RSSI_{cl}$ (dBm)	Estimated Distance$_{ah}$ (m)	Estimated Distance$_{cl}$ (m)	Absolute Error$_{ah}$ (m)	Absolute Error$_{cl}$ (m)
1	0.5674	-42.51	-41.23	0.3443	0.2460	0.2231	0.3214
2	0.6038	-45.82	-47.11	0.9850	1.0727	0.3812	0.4689
3	1.1349	-46.44	-48.16	1.6227	1.6563	0.4878	0.5214
4	1.4547	-47.15	-45.96	1.9777	0.8426	0.5230	0.6121
5	1.7023	-46.01	-50.98	1.0313	2.4571	0.6710	0.7548
6	1.7602	-45.62	-51.65	1.0146	2.5704	0.7456	0.8102
7	1.9431	-50.55	-46.44	2.7485	0.9465	0.8054	0.9966
8	2.1661	-51.21	-53.52	3.0892	3.2126	0.9231	1.0465
9	2.2698	-52.43	-54.18	3.3236	3.4246	1.0538	1.1548
10	2.6386	-53.22	-47.39	3.7719	1.3930	1.1333	1.2456
11	2.8372	-46.21	-56.87	1.6111	4.1483	1.2261	1.3111
12	3.1375	-46.88	-57.74	1.7829	4.5274	1.3546	1.3899
13	3.4047	-56.82	-58.18	4.8669	4.9186	1.4622	1.5142
14	3.6609	-57.60	-59.66	5.1616	5.3297	1.5010	1.6688
15	4.5396	-58.22	-60.41	6.2128	6.2811	1.6732	1.7415
16	4.7348	-59.35	-61.58	6.4364	6.6171	1.7016	1.8823
17	5.6745	-53.56	-55.43	3.9024	3.6836	1.7721	1.9909
18	5.8318	-61.23	-55.89	7.7248	3.8004	1.8930	2.0314

method, five nearest values are selected. Besides, for the KF method, the process noise is chosen 0.2, and for the RF method highest five decision trees are created. It can be seen from figure 5.4 in both rooms that the proposed KNN data filtering

approach gives errors under the KF and RF methods. The error differences are substantial at every position between the KNN data filtering approach and the other two approaches in every room. However, the error difference between KF and RF is not too large. The highest localization errors for KNN, KF, and RF methods in the 'ah' are 1.8930 m, 3.1412 m, and 3.5517 m and in the 'cl' are 2.0314 m, 3.3557 m, and 3.6170 m. With the above formations, the experimental results show that the KNN technique is more suitable for the proposed algorithm than KF and RF.

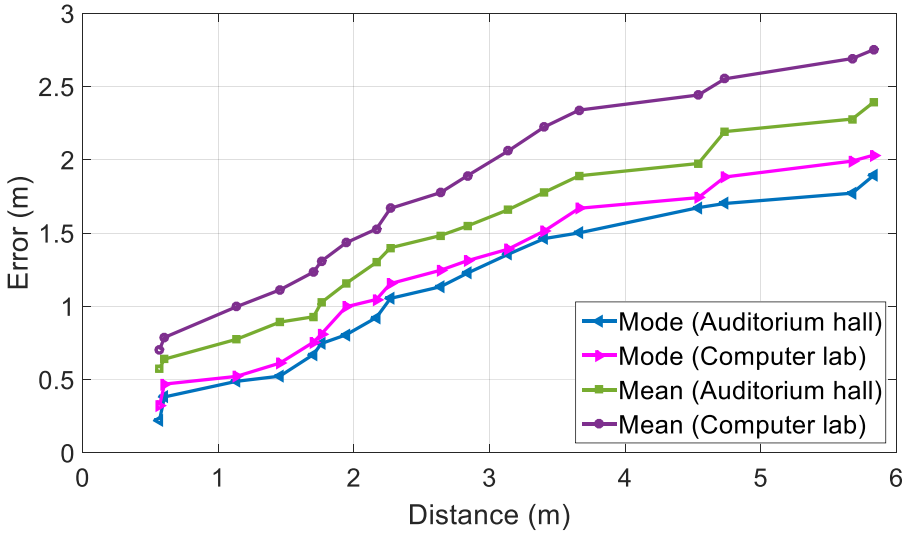

Figure 5.3: Comparison of location errors for special RSSI values in different environments.

Table 5.3: Comparison of the highest errors in different rooms

	Auditorium hall		Computer lab	
Algorithm	Static	Dynamic	Static	Dynamic
Proposed	1.8930 m	2.5621 m	2.0314 m	3.2161 m
SD-KNN	3.2261 m	3.7761 m	3.5159 m	4.4412 m
SRL-KNN	3.5421 m	4.3422 m	4.1120 m	5.0147 m
Distr-UKF		2.7911 m		3.7412 m
Min-Max-APS		4.1221 m		4.9247 m

The above experimental results assure that with the mode RSSI values and KNN data filtering method, the proposed algorithm provides much higher accuracy.

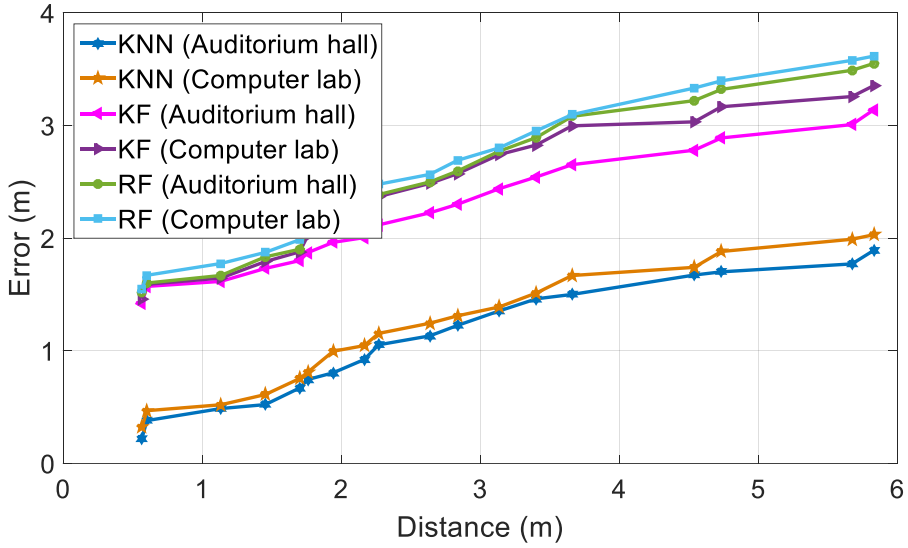

Figure 5.4: Comparison of location errors for different data filtering approaches in different environments.

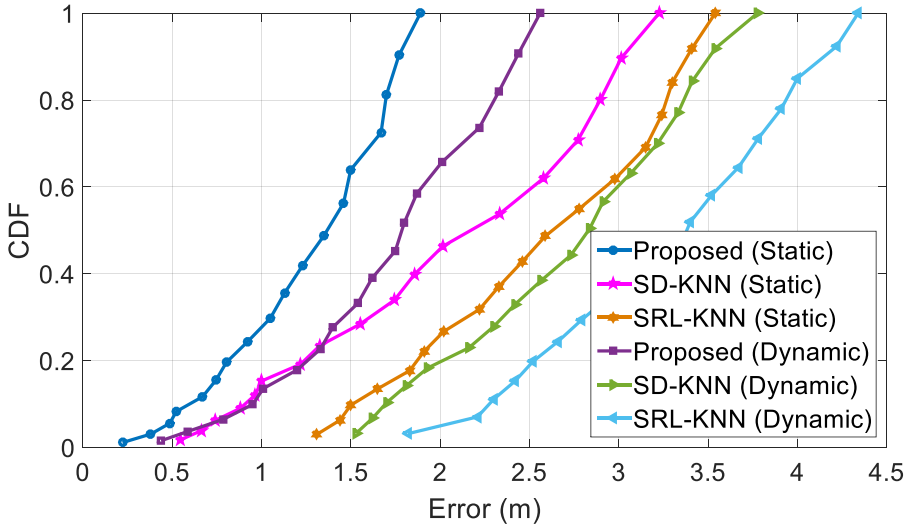

Figure 5.5: Comparison between algorithms for location accuracy at the auditorium hall in terms of CDF.

Further, for more satisfactory evaluations considering the different points of view, the proposed algorithm is compared considering tasting with the other two state-of-the-art KNN-based algorithms (i,e., SD-KNN [82] and SRL-KNN [33] algorithms) that maintain the same test environments for static and dynamic sce-

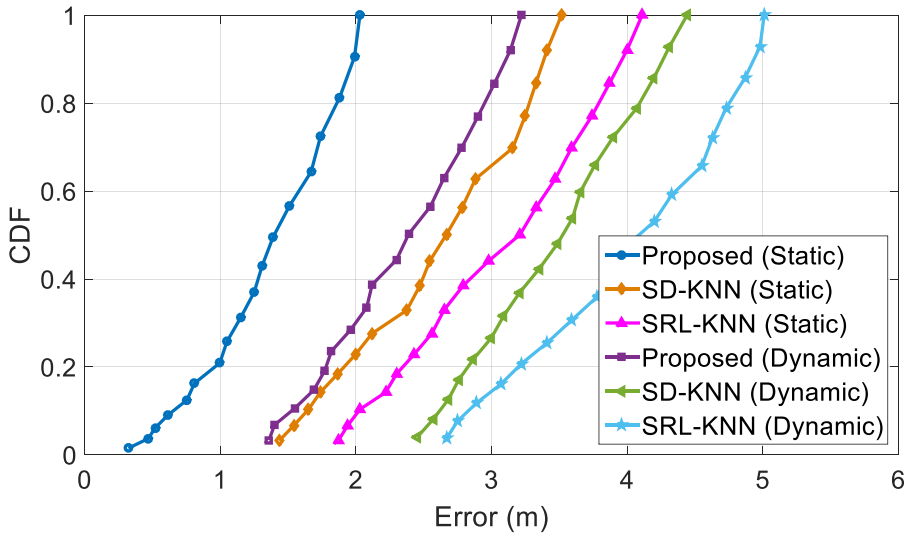

Figure 5.6: Comparison between algorithms for location accuracy at the computer lab in terms of CDF.

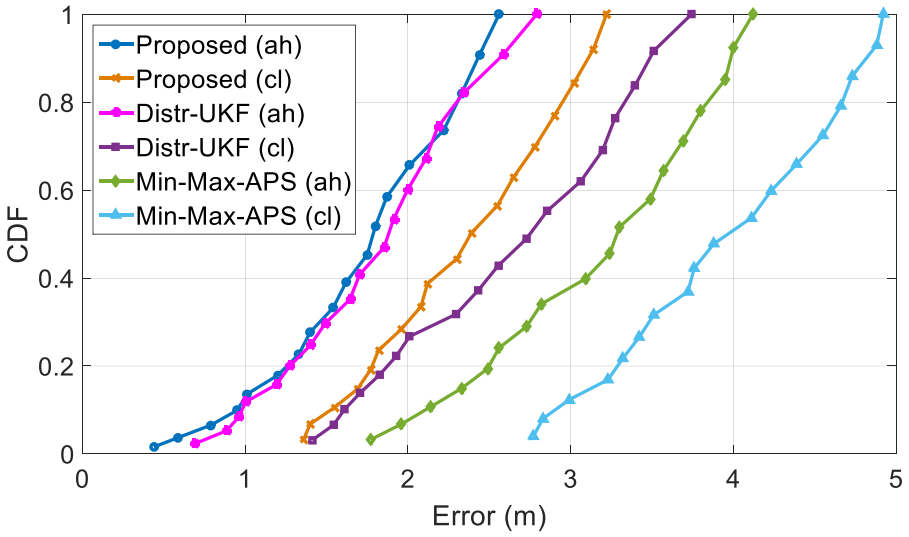

Figure 5.7: Comparison between algorithms for dynamic location accuracy in terms of CDF.

narios. Even in every algorithm, the fingerprinting method has been used. The precision is measured by the cumulative distribution function (CDF) for the positioning error, which is the difference between the actual and estimated locations. The rank RSSI value has been used in the SD-KNN approach. On the other

hand, the mean RSSI value has been used in the SLR-KNN method. Figure 5.5 illustrates the comparative scenario of the proposed algorithm with SD-KNN and SRL-KNN algorithms. It is observed that in the 'ah', the accuracy of the proposed algorithm is very high than SD-KNN and SRL-KNN algorithms in the static situation. However, the precision of SD-KNN is much close to some initial positions of the proposed one, but when the distances grow, its errors reach an extreme level. In contrast, the errors of SRL-KNN stay bigger than others. If we consider the dynamic situation of the proposed algorithm, it will be observed that some initial positions are much close to the static positions. However, for the growing conditions, its errors are also increased, whereas the dynamic errors of others algorithms are comparatively huge. Similarly, figure 5.6 depicts the proposed algorithm again achieving higher precision than others in the 'cl' at static and dynamic situations. To further verify the capabilities of the proposed algorithm, it is compared with the other two state-of-the-art algorithms, including Distr-UKF [88] and Min-Max-APS [86], with the reasonable parameters in dynamic situations, which can be seen in figure 5.7. If we consider the scenario of 'ah', it can be observed that the accuracy of the proposed algorithm and the Distr-UKF algorithm are almost nearest to each other. Even for some positions, the Distr-UKF achieves relatively higher accuracies than the proposed one. On the other hand, if we consider the scenario of 'cl', it can be seen that for some initial positions, the accuracies of the proposed algorithm and Distr-UKF algorithm are very close, but when the distances increase, it makes significant differences where the accuracies of the proposed algorithm are much better than the Distr-UKF method. In contrast, the accuracies of the Min-Max-APS algorithm in both 'ah' and 'cl' are very low. Its situations continuously maintain huge disparities from the other two algorithms.

The largest error observation for each algorithm can be seen in TABLE 5.3. The comparative results in static states show that the largest error percentage of the proposed algorithm in 'ah' is 32.46%, which is very small than the SD-KNN and SRL-KNN algorithms. Those have the highest error percentages, 55.32%, and 60.74%, respectively. On the other hand, in 'cl', the error percentage of the proposed algorithm is 34.83%, which is also very small compared to SD-KNN

(60.29%), and SRL-KNN (70.51%). The comparison of dynamic state in 'ah' illustrates the largest error percentages of the proposed algorithm and Distr-UKF are very close, i.e., 43.93% and 47.86%, respectively, where SD-KNN (64.75%), SRL-KNN (74.86%), and Min-Max-APS (70.68%) generates more substantial errors percentages. In the 'cl', the largest dynamic relative error percentages of the proposed (55.15%) and Distr-UKF (64.15%) are comparatively bigger than 'ah'. However, the largest error percentages of SD-KNN (76.15%), SRL-KNN (85.99%), and Min-Max-APS (84.45%) are comparatively huge. The assessment shows that for various scenarios, the proposed algorithm can produce a better performance than other algorithms as well as its robustness is very high. From this table, it also observed that (i) the largest errors of the proposed algorithm are always under the SD-KNN and SRL-KNN approaches in static conditions for both rooms, (ii) the largest errors of the proposed algorithm are always close to the Distr-UKF algorithm in dynamic states compared to the SD-KNN, SRL-KNN and Min-Max-APS algorithms, (iii) the largest static or dynamic errors of both algorithms in 'cl' are higher than 'ah' for the same state due to the increase in noise materials, (iv) the largest dynamic errors for these algorithms in 'ah' are greater than the largest static errors in 'cl', (v) the presence of outdoor radio devices do not keep a significant impression to the indoor measurement systems.

5.4.1.1 Throughput of Algorithm

For this experiment, a laptop Intel® Core™ i3-2310M CPU @ 2.10 GHz with 4.00 GB RAM and 64-bit operating system is used, where the laptop compiles a different size of the data packets to calculate the performance of the proposed algorithm. The throughput of any algorithm can be calculated by

$$Throughput = \frac{TS}{TT} \tag{5.6}$$

where TS is the total size of the data packets and TT is the total execution times of compilation. Different sizes of data packets, i.e., (214570/250800/292300) bytes, are used to observe the outcomes. It is seen that the throughputs of the

proposed algorithm are 104.77 Kbps for 214570 bytes data packets, 81.64 Kbps for 250800 bytes data packets, and 63.43 Kbps for 292300 bytes data packets, respectively.

5.5 Conclusions

This chapter presents a novel Wi-Fi indoor localization algorithm utilizing the RSSI fingerprinting methods. The proposed algorithm is generated by the analysis of characteristics of RSSI outcomes considering various environmental scenarios. Two APs are used to estimate the locations of the RP (smartphone) on the indoor premises. A nonlinear attenuation model has been employed to represent the relationship between distances and RSSIs. Using the positions of two APs, situated at the corner and center, and the distances between APs and RPs, smartphone locations at different RPs in a half portion inside a room are estimated. The experimental and simulation results for two different scenarios confirm that the positioning capability of the presented algorithm is significantly more accurate and beneficial compared to other existing approaches, considering the RSSI-based ranging technique. Thus it could be utilized extensively in the indoor environment as a complement to current localization systems for various positioning applications.

Chapter 6

Signal strength based Real-Time Position Tracking of Vehicles

In the chapter, an signal strength-based position tracking [51] scheme of the vehicle has been investigated. The next-generation vehicular tracking applications on the road bring many benefits, including aided travel time estimation, traffic trajectory observation, and quick congestion control. To meet such requirements, adopting the positioning system with wireless received signal strength (RSS) is a cheap, reliable, simple, and robust solution because RSS indicates the current condition of the signal by geographically overlaying across a region. Considering the usefulness of RSS, this paper has investigated an enhanced vehicle tracking scheme incorporating the environmental issues in the driving motions, where consecutive Base Stations (BSs) are deployed nearby the road to track the position of vehicles moving through different road lanes. From the rooftop, the antenna of each vehicle radiates the omnidirectional signals [42] that exploit by the nearby BSs antennas. Consequently, the data analysis platform associated with the network recognizes the current position of each vehicle using the received RSSs in different BSs by their identity (ID). In the road junction, vehicles can take turns to change their road where for vehicle positioning, multiple BSs may be required. Therefore, to improve the evaluation accuracy, the multiple BSs-based approach

has been incorporated. The change in a vehicle's position is determined by observing the change in respective RSSs received by successive BSs.

6.1 Background

With autonomous technologies, modern vehicular networks are now becoming more intelligent by developing new traffic monitoring [53] schemes. Among different traffic handling strategies, the position tracking of the vehicle achieves dramatic interest due to its several benefits and feasibilities. The procedure can regularly be applied not only for safety precautions but also for information exchanges. In the proposed framework, the RSS-based [85] position tracking scheme has been introduced to reduces any kinds of difficulties, including system complexity, signal blockage, computational overhead, and power consumption, can mitigate significantly. In this strategy, while a vehicle moves along the road, consecutive tracking BSs of it are subsequently changed. Since vehicles sometimes move on a straight multi-lane road in any direction, the change in a vehicle's position is determined by observing the change in respective RSSs received to successive BSs. Similarly, in the same manner, BSs track the vehicles which move in the opposite direction.

6.2 System Model

Consider a vehicular network infrastructure [76], where BSs are planted on the median strip of the bidirectional road, maintaining equal intervals. The antenna, installed on the top of each BS has the same sensing coverage area and equal altitude from the road surface. There are different lanes on the road for the vehicles' movement, and many roads meet at the junctions. When a vehicle moves through different sensing regions of successive BSs, the antenna installed on it (i.e., access point (AP) [36]) radiates the signal, which is received by different BS antennas (i.e., stations (STAs) [3]). By observing the RSS samples, the associated data analysis platform with the BSs network tracks the direction of moving vehicles.

Since the movement of vehicles bound to different lanes of straight road, RSS change is negligible for slight displacement in the sides.

Considering the height of the BS antenna, the shape of a vehicle is insignificant. The coverage area of a BS is πR^2 for radius R. Since, in most cases, vehicles move in a particular direction. Thus their positions can be tracked using the nearer BSs. In the following, the proposed vehicle tracking procedure has been explained systematically.

Assume that a vehicle is moving on a road from the point R_1 to R_2, through the lane L_1 (Fig. 6.1). At a certain time, the position of the vehicle is P. The BSs nearest to P are BS_1, BS_2 and BS_3 (according to Fig. 6.1). The height of each BS is h. At a certain time t, we have to find the position $P(x, y)$ of the vehicle.

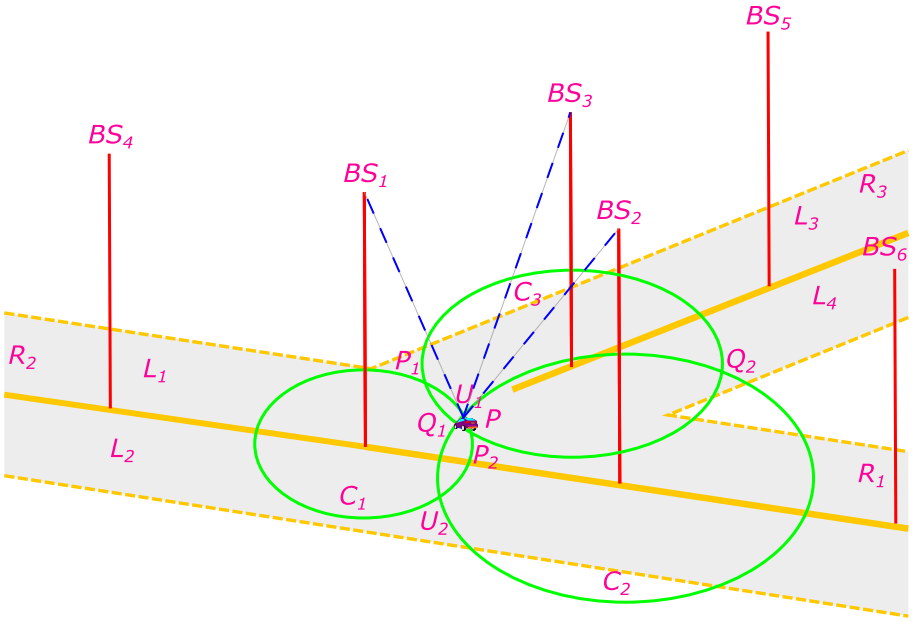

Figure 6.1: Illustration of the vehicle tracking system using BSs in the junction.

Consider a BS receiving the RSS from the vehicle at a certain time t. At the particular time t, let A be the position of the antenna of the BS, B be the position of the BS, and C be the position of the vehicle (see Fig. 6.2). Then, the height of the BS is denoted as AB, which is equal to h. AC denotes the distance of the vehicle from the antenna of BS that is equal to d, and the distance of

the vehicle on the ground from the bottom of the BS is r, which is denoted by BC. Then, if a circle of radius r and center B is drawn, then the circle is called signal strength's coverage circle, which is denoted as C. This radius r can be determined by the Pythagorean theorem applied on the right angle triangle ΔABC as $r = \sqrt{(d^2 - h^2)}$, where h is the height of the BS and d is the elevation distance of the vehicle from the position of the antenna B.

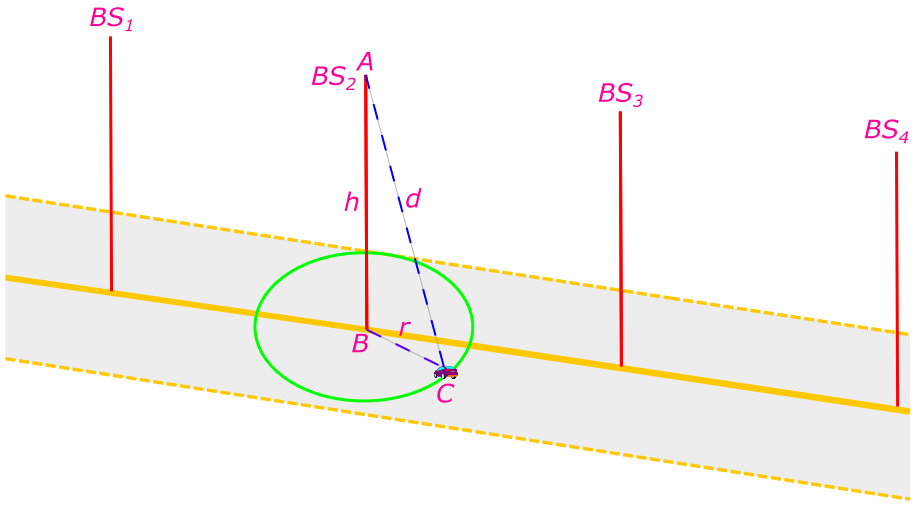

Figure 6.2: Illustration of the vehicle tracking system using a single BS.

This d can be measured by, $d = d_0 \times 10^{\frac{(rss_0 - rss_p)}{10\gamma}}$ where d_0, rss_0, and γ are the environmental parameters and rss_p is the measured RSS value.

6.3 Tracking Algorithm

In the following, the tracking algorithm has been investigated to estimate the position of each vehicle between the BSs. The data analysis platform associated with all BSs determines the vehicle's position using the BSs identities.

Let at any time instance t, for a particular vehicle we get n ($n \geq 3$) different signal strength's sensing coverage circles C_i $i = 1, 2, \ldots, n$ (in Fig. 6.3, there are 3 coverage circles C_1, C_2, and C_3). Consider 3 coverage circles C_1, C_2, and C_3 among n circles. Compute the position of the pair of intersecting points for

the pair of circles C_1, C_2 and C_1, C_3 (in Fig. 6.3 P_{12}, Q_{12} and P_{13}, Q_{13} are the pair of intersecting points for the pairs of circles C_1, C_2 and C_1, C_3 respectively). Then, calculate the distances for each pair of intersecting points. Among these distances, consider the minimum distances (if there exists more than one pair for which minimum distance occurs, then break the tie arbitrarily). Let P_1 and P_2 be the pair of points for which minimum distance occurs. These P_1 or P_2 can be the possible correct position P of the vehicle.

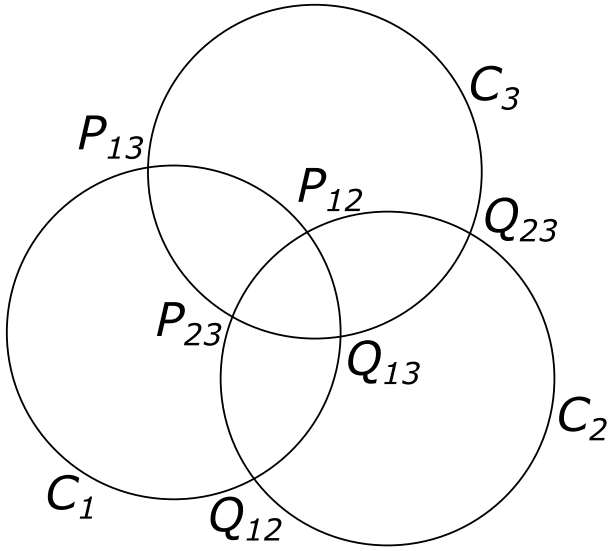

Figure 6.3: Illustration of three coverage circles of BSs.

Let us consider the set of all possible correct positions and name it as $\mathbb{S}$. Initially, $\mathbb{S}$ consists of those two points P_1 and P_2 calculated before. Consider any one point from the set $\mathbb{S}$ and name it as R, $i = 2, \ldots, n-1$. Compute the intersecting points for the circles C_i and C_{i+1}, $i = 2, \ldots, n-1$. Let the intersecting points are S_i and T_i for $i = 2, \ldots, n-1$. Then calculate the distances $\overline{\mathrm{R_i S_i}}$ and $\overline{\mathrm{R_i T_i}}$. Consider the point between S_i and T_i for which minimum occurs and named it as P_{i+1}. Include P_{i+1} in the set $\mathbb{S}$. Thus, proceeding in a similar manner, we get the set $\mathbb{S}$ with n points $\mathbb{S} = \{P_1, P_2, \ldots, P_n\}$. Compute the center of gravity (C.G.) of those n points. This is the desired destination point $P(x, y)$, which is the location of the vehicle at a particular time instance t.

Algorithm 6.1 Position Tracking

procedure TRACKING
    /* BS_is be n Base Stations, $i = 1, 2, \ldots, n$ */;
    Input: $B_i(x_i, y_i) \longleftarrow$ location of BS_i, $i = 1, 2, \ldots, n$;
    $d_i \longleftarrow$ distance (noisy) of vehicle from the antenna of BS_i estimated at an instant t;
    Output: $P(x, y)$ estimated location of the vehicle at time t;
    Compute radii r_is for n coverage circles;
    Compute n coverage circles C_is with center $B_i(x_i, y_i)$ and radius r_i, $i = 1, 2, \ldots, n$;
    Compute intersecting points: for the pair of circles C_1, C_2, and C_1, C_3;
    For each pair of the intersection points, compute distances;
    Consider the minimum distance; break the tie arbitrarily;
    Let P_1 and P_2 be the pair points with the minimum distance;
    $\mathbb{S} \longleftarrow \{P_1, P_2\}$ /* $\mathbb{S}$ is the set of possible correct positions */;
    for $i = 2$ to $(n - 1)$ **do**
        Select an arbitrary point from $\mathbb{S}$, rename it as R_i;
        Compute the intersecting points of C_i and C_{i+1}, say S_i and T_i;
        Compute the distances $\overline{\mathrm{R_iS_i}}$ and $\overline{\mathrm{R_iT_i}}$;
        Find $d = min\{\overline{\mathrm{R_iS_i}}, \overline{\mathrm{R_iT_i}}\} = \overline{\mathrm{R_iP_{i+1}}}$, $P_{i+1} = S_i$ or T_i;
        $\mathbb{S} \longleftarrow \mathbb{S} \cup \{P_{i+1}\}$;
    end for
    Compute $P(x, y) \longleftarrow$ center of gravity of n points P_is of $\mathbb{S}$;
end procedure

6.4 Conclusions

In this chapter, an RSS-based position tracking scheme has been investigated for vehicles considering moving scenarios using the coverage areas of various BSs. The data analysis platform associated with every deployed BS determines the vehicle's position in every iteration utilizing the exploit RSSs to single or multiple BSs. The proposed RSS-based vehicle tracking scheme is more simple, reliable, robust, and can be applied as a complement to the current GPS system. Considering environmental anomaly concerns, in the future, the scheme can be utilized for online decision-making to reduce on-road traffic jams.

Chapter 7

Sensing Capable Multi-hop Strongly Connected Network

This chapter presents a sensing-capable multi-hop Wi-Fi router [15] network framework, where the multi-hop [20] routers will be installed in different locations and will be connected to one another wirelessly through the ring network topology, where inside a router, through wire connection AP transmits a query to the STA, but the query response will not come from STA to AP through the wire, it will move from STA to AP wirelessly with a different path. The path is strongly connected. Moreover, by connecting to any router with a smartphone, the user can send the query [80]. To effectively deal with the query through the multi-hop network [27], the cost-effective sensing-capable multi-hop router network is a compelling choice for a large number of people, which not only reduces the overall costs of the network but also saves energy because this router can work long times with a small power battery backup.

7.1 Background

In wireless sensor networks (WSNs) [96], multi-hop communications play a significant role because, with the multi-hop router, the range of the network can be expanded to a particular direction without increasing the sensing coverage area of any router, which does not only reduce energy consumption but also increase network capabilities according to the requirements. Even connection loads can be efficiently distributed between multiple routers. Due to their small size, wireless routers can easily be portable from one place to another and can be taken into operation in any location for different purposes. Besides, it can be integrated as a part of the existing network infrastructure to meet the users' requirements. For its various functionalities, it can comfortably use in indoor as well as outdoor regions. However, for the requirement of high data throughputs considering massive users' demands, the wireless multi-hop router fails to achieve desired performance due to channel shortage, limited bandwidth, processing complexity, and computational overhead. So a large part of the conventional network runs over wire cables [46], which is very costly to meet small or personal network demands. In addition, to install and maintain the wired network, experienced technicians are required, but their services do not always remain freely available. Even every application does not demand the requirement of an expensive network, especially those networks which are built for lower data transmission. In contrast, traditional Wi-Fi routers are not developed with sensing capabilities, which restricts their applicability. This section focuses on developing cost-effective sensing capable multi-hop routers'.

7.2 System Design

In this work, we developed a cheap and simple multi-hop router with sensing capabilities using some wireless modules easily available in the market to construct a offline network for a surveillance system. Among the low-price radio technologies, Wi-Fi is more popular than relevant technologies such as Bluetooth

and ZigBee due to its unique features, e.g., wide coverage, high data throughput, large bandwidth, and minimum installation costs. Even common commercial Wi-Fi devices operate on 2.4 GHz unlicensed ultra high frequency (UHF) and are generally known as industrial, scientific, and medical (ISM) bands. Therefore, to develop a multi-hop router, we use Wi-Fi supporting micro-controller unit (MCU) compatible [57], two wemos D1 R2 modules [39], and programmed one as AP and another as STA to establish the wireless connection between routers. In each router, the AP is the gateway to the network, which allows external wireless devices and the STA of other routers to use the network interface. On the other hand, in a router, an STA is used to increase the network range by connecting to another router wirelessly. Typically, it is very hard for a wemos D1 R2 module to do both works simultaneously as AP+STA. Because in this case, data management overhead and computational complexity will be gradually increased when concurrent data from multiple sources passes through this module. As a result, the communication process can be ceased by the hang of the network. So to leverage the network capabilities, individual mechanisms are used in AP and STA.

To each wemos D1 R2 module, by default, the same wireless channel is used to exchange data through carrier sense multiple access with collision avoidance (CSMA/CA) protocol [22] (half duplex), which can create a situation of data collision when inside a router, both AP and STA simultaneously transmit and receive different wireless data. Therefore, individual data need to pass through different channels to avoid the collision. Moreover, for a router inside communication between AP and STA, there require a wire protocol, which can successfully mitigate data loss because compared to a wireless connection, the data loss of wire connection is negligible. In a wemos D1 R2 module, to communicate with other modules, there only have three wire protocols (figure 7.3), including universal asynchronous receiver/transmitter (UART), inter-integrated circuit (I2C) [73], and serial peripheral interface (SPI) [7], whereas, for communication between AP and STA, the UART [40] is the compelling choice due to its programming codes' simplicity and require only two jumper wires to transmit data from the source to destination. In contrast, serial clock line (SCL) and serial data line

(SDA) based I2C data exchange policy implementation between AP and STA through programming codes is very difficult and may not be successfully executed. Besides, the master in slave out (MISO), master out slave in (MOSI), and serial clock (SCK) enabled SPI data transmission mechanism also face similar problems as I2C. However, both UART and I2C are half duplex, but SPI is a full duplex protocol.

To enable each router to be sensing capable, required to include some sensor on it. Nevertheless, in a router, both AP and STA will face a large number of conditional issues on their programming codes regarding data exchange. Even each AP has to manage multiple wireless connections through programming. Thus AP cannot tolerate such a burden. Although each STA has lower computing pressure than AP, but when sensors are added to it, it may produce the worst performance. So neither AP nor STA is suitable for including sensors on it. Therefore, another external module is required, which can perfectly handle all connected sensors' communications. Consequently, an Arduino Uno board is included in each router as a controller of sensors. The controller is wire connected to STA. To communicate between STA and controller, there have only two remaining protocols, i.e., I2C and SPI. However, the programming codes of I2C is more simple than SPI for STA and controller communication. So, the I2C protocol is used, where its programming code is developed to obey the requirement regarding the sensors. Both modules are programmed using Arduino integrated development environment (IDE) software. The individual external users can observe the current outcomes of sensors of other routers by connecting to any router of this multi-hop network with their smartphone. To successfully manage this system, an APP has been designed for the smartphone [29]. However, to access a router, there needs to include a password authentication system such that information can be secured efficiently. Each sensor is wire connected to the controller. In each router, the same sensors are used for various purposes, such as relays used to light, fan, etc., to turn on/off them, Hc-Sr501 sensor used for motion detection, MQ-2 used for fire recognition, MQ-5 for gas detection, MQ-3 for alcoholic activity detection and LM393 for sound discovery. To the communication mechanism, when an AP receives data from any source, it forwards this data to the

STA through the wire connection inside the router and to the destination router of the query. STA sends the query to the wire-connected controller and receives the response, which will be sent to the source AP through another path. Meanwhile, a liquid crystal display (LCD) can be included in each router to display the information, and power will be given to each router by a lithium-ion battery. Fig. 7.1 illustrates the communication overview of the proposed sensing-capable router.

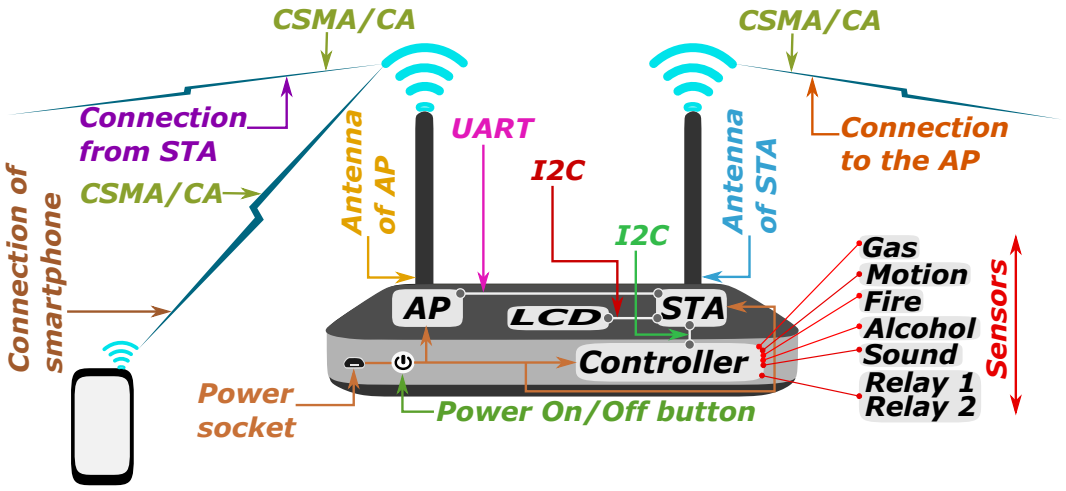

Figure 7.1: Framework of sensing capable multi-hop router.

7.3 Strongly Connected Theorem

In this work, we have considered a set of routers. Each router consists of an AP and an STA. There is an internal wire connection from the AP to the STA of a router. There is also a controller which communicates with the STA. There is an external wireless connection from the STA of a router to the AP of another router. Consider a router as a vertex and the connection from the STA of a router to the AP of another router as a directed edge. Our target is to form a strongly connected directed graph. A strongly connected directed graph is a graph whose edges are directed, and any vertex is reachable from any other vertex. We have considered another condition that an STA of a router can connect only one AP

of another router. We will show that the graph must be a directed cycle. The connection scenario of the network is described in Fig. 7.2.

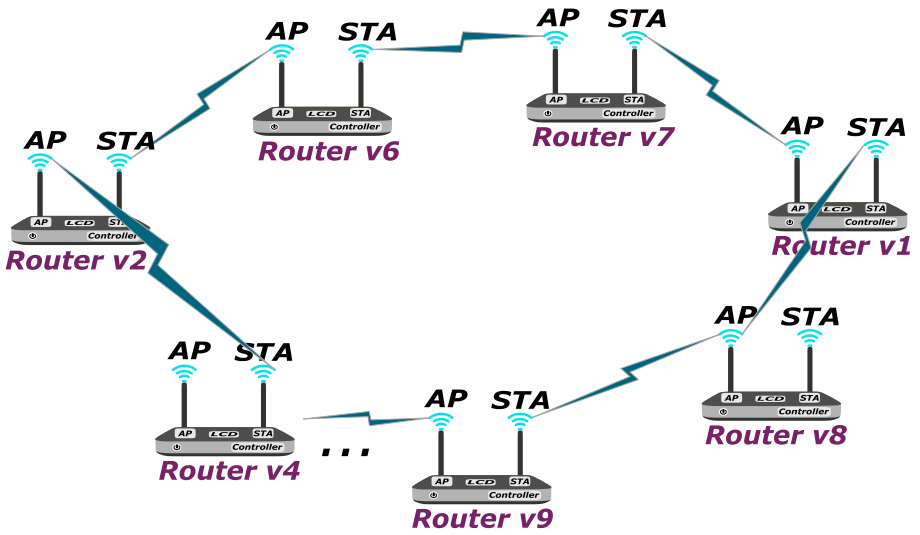

Figure 7.2: Strongly connected scenario of the network.

Theorem : According to our conditions, the graph is strongly connected iff it is a directed cycle.

Let the graph is strongly connected and { *Router* v_1, *Router* v_2,..., *Router* v_n } be n vertices of the graph. Since the graph is strongly connected, there is a directed path from *Router* v_1 to *Router* v_2. Discard all the vertices which appear on the directed path from the vertex set. Now find the directed path from *Router* v_2 to the least indexed vertex in the vertex set. In this directed path, all the vertices are different from the discarded vertices. Otherwise, there will exist a vertex from which more than one edge exit. It is impossible, according to our assumption. In this way, we will get a finite number of directed paths. Combine these directed paths and give a directed edge from the last discarded vertex to *Router* v_1. This will form a directed cycle.

Conversely, let the graph be a directed cycle. Any vertex is reachable from any other vertex. Thus the graph is strongly connected.

7.4 Algorithmic Statement

This sensing-capable multi-hop router is composed of mainly three components, i.e., AP, STA, and controller, to manage the network system perfectly. Their working methods are described by Algorithm 7.1, Algorithm 7.2, and Algorithm 7.3, respectively.

Algorithm 7.1 AP

```
1: setup:
2: ID // Identity of AP; Port number // Serial port; dataStr // Variable to store the data
   packet (pkt); Connections limit // Maximum number of STA connection;
3: end setup
4: loop:
5: if an STA try to connect to this AP then
6:     if no free slot is available for allocation then
7:         Reject the new connection;
8:     end if
9:     Let i^th slot of AP is available for allocating STA;
10:    STA connects to i^th slot of AP;
11:    Obtain pkt from i^th slot are stored in dataStr;
12: end if
13: if dataStr is non-empty then
14:    if the destination of pkt is the wire connected STA then
15:        Send the pkt to the wire connected STA of the AP;
16:    else
17:        Forward the pkt to the appropriate wireless STA;
18:
19:    end if
20: end if
21: end loop
```

7.5 Network Protocols

For wireless communications among modules, IEEE 802.11 standard is defined as a distributed coordination function (DCF) for sharing access to the medium, based on the CSMA/CA protocol with a binary exponential backoff algorithm. In CSMA/CA, a module can sense the channel before sharing its data packet. First, it listens to the channel to determine whether some other module is transmitting data or not. To avoid collisions, modules attempt transmission only when

Algorithm 7.2 STA

```
1: setup:
2: Port number // Serial port; dataStr // Variable to store data packet (pkt); AP-list // A
   predefined list of APs with IDs to form a network;
       availableAPs // A list of APs whose signals are available to the STA;
3: end setup
4: loop:
5: if pkt is available from the controller or the wired AP then
6:     Receive pkt is stored in dataStr;
7: end if
8: CheckConnectivity(): // Check for a connection to the AP;
9: for each AP ∈ AP-list do
10:    if AP ∈ availableAPs then
11:        ListenAP(): // Listen AP with appropriate ID and port;
12:    end if
13: end for
14: if dataStr is non-empty then
15:    Deliver the pkt from dataStr to its destination (dst);
16:    if dst is the STA itself then
17:        Send the pkt to the controller;
18:    else if pkt is available from the wireless AP then
19:        Send pkt to the wired AP;
20:    else
21:        Send pkt to the wireless AP; // pkt is received from the wired AP;
22:        if the wireless AP is disconnected then
23:            ConnectionRequest(): // Request to connect to the wireless AP;
24:        end if
25:        On connection, pkt is transmitted to dst;
26:    end if
27: end if
28: end loop
29: function ListenAP()
30: if wireless AP is found then
31:    Return true;
32: end if
33: end function
34: function CheckConnectivity()
35: if any wireless AP is available from the routing table to the STA then
36:    This AP will be added into the list availableAPs;
37: end if
38: end function
39: function ConnectionRequest() // STA want to connect the target AP;
40: if STA is disconnected from the AP then
41:    Try to reconnect the AP;
42: end if
43: end function
```

Algorithm 7.3 Controller

```
1: setup:
2: strReceive // Variable to store data packet (pkt) received from STA; strRequest // Variable
   to store pkt received from a sensor;
3: end setup
4: loop:
5: ReceiveEvent(): // Controller listens STA to receive pkt from it;
6: RequestEvent(): // Controller listens STA for forwording pkt to it;
7: if a pkt is found for a sensor then
8:     Input mode // Obtain pkt from the sensor;
9:     Insert sensor's pkt to the strRequest;
10: end if
11: if a pkt is found for a relay then
12:     Output mode // Forward pkt to the relay;
13:     Deliver STA's pkt by the strReceive;
14: end if
15: if strRequest is non-empty then
16:     RequestEvent(): // strRequest is sent to STA;
17: end if
18: if strReceive is non-empty then
19:     ReceiveEvent(): // strReceive is sent to relay;
20:     Relay starts to control a device;
21: end if
22: end loop
23: function ReceiveEvent()
24: Receive the pkt to strReceive from the STA;
25: end function
26: function RequestEvent()
27: Send the pkt from strRequest to the STA;
28: end function
```

the channel is sensed idle. If another module is heard with message sharing, it waits for a period until it listens to a free channel for communication. Therefore CSMA/CA is considered a contention-based access protocol as well as it is simple, feasible, robust and mainly used for dynamic network topology. Moreover, CA is introduced, among other wireless approaches to minimize the impact of hidden and exposed terminal problems. This protocol enabled to transmission and receive data with point-to-point (P2P) and point-to-multipoint (P2MP) group operations. The CSMA/CA consists of an RTS/CTS access mode. The protocols for the wemos is presented in Fig. 7.3.

To communicate between two modules, the UART is a low-data-rated generating

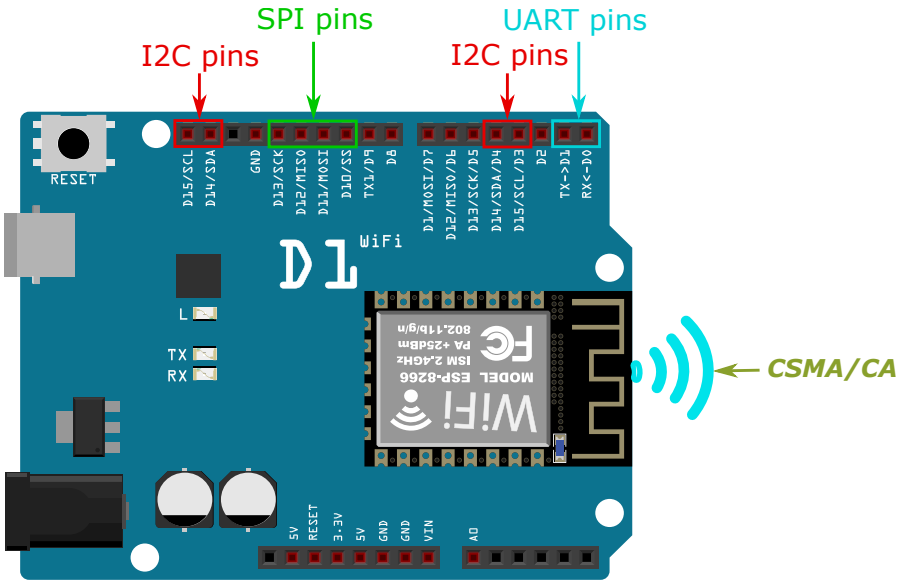

Figure 7.3: UART, I2C, and SPI pins of a wemos D1 R2.

protocol. However, the efficiency of UART is very high compared to other inbuild protocols defined in the modules. The UART is a form of serial communication of digital data since all data is transmitted as sequential bits. It requires only two wires for communicating from source to destination. In this protocol, the T_X pin of the transmitter is directly connected to the R_X pin of the receiver and vice versa. Each transmitting data frame consists of one start bit, a maximum of 9 data bits, one parity bit, and one stop bit. After detecting a start bit, the receiver begins to read the incoming bits at a specific frequency known as the baud rate. Both modules must operate at about the same baud rate. The parity bit informed the transmitter whether any data had changed during transmission or not.

The I2C is a synchronous communication protocol. It can connect multiple masters to multiple slaves. However, to communicate between two modules, only one master and one slave are used. I2C is a two wires interface, one is the SDA, and the other is the SCL. The SDA line sends and receives data for the master and slave, whereas the SCL line carries the clock signal. The data frames begin with one start bit and end with one stop bit. For identifying each module, there has

a pre-defined address of 7 or 10 bits. The address bits are followed by a control (read/write) bit. This read (R) or write (W) bit determines whether the master module writes to or reads from the slave.

7.6 Application Scopes

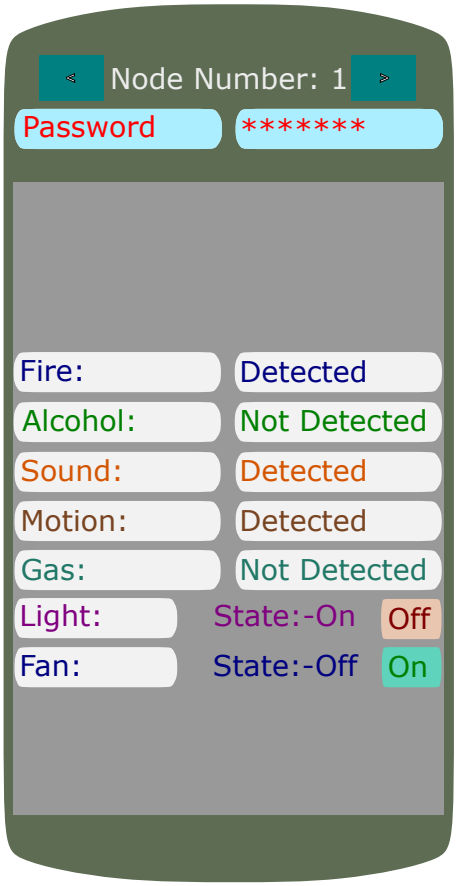

Figure 7.4: Background of the smartphone APP.

This multi-hop network can easily be made in any place with a simple setup, as each router is very small in size. A personal and temporary network can be formed with a few routers efficiently. Each router can be attached to the network without any fixed infrastructure. It is useful for both rural and urban communication. This communication process is very comfortable because any instruction can be

sent through the smartphone APP, which is drown in Fig. 7.4.

To the indoors, the network is usable in industries, homes, hospitals, hotels, restaurants, shopping malls, etc. Moreover, for outdoors, the network is usable in agriculture, forests, mountains, rivers, deserts, etc. In the case of a natural disaster, i.e., earthquake, flood, fire, etc., the network will be helpful. Also, different educational work can be organized using this multi-hop network.

7.7 Conclusions

In this chapter, to send the query using the smartphone, a sensing-capable multi-hop routers network framework is planned based on the ring topology. To make each router, according to the requirement, different cost-effective modules are used and programmed such that they can do different tasks to manage the network datum. There are limited inbuilt protocols in these modules, which have different programming challenges to establish various types of connections. However, for developing this sensing-capable multi-hop router, best of our knowledge, proper protocols are chosen according to the working functionality, which optimizes the system performance.

Chapter 8

Conclusions

Wireless sensor networks (WSNs) have been used in various applications such as surveillance, target tracking, habitat monitoring, medical treatment, space exploration, etc. Since sensing and communication is the main operation in these networks, it is important to know the location at which device readings originated or the target is detected. Apart from this, localization information of devices is inevitable for geographical routing, data aggregation, and tracking services. Thus, localization has been studied as a critical research issue in WSNs. Besides, in this thesis, we develop a sensing-capable multi-hop routers communication network for surveillance systems. To develop the surveillance systems, a strongly connected ring network has been designed, as well as to communicate between different modules, proper protocols and programs are used.

8.1 Our Contributions

We first proposed the different techniques for position localization based on the RSS approach. Then, a multi-hop communication network strategy is presented for the surveillance system.

In chapter 3, an efficient distance estimation technique has been proposed using the receiver's angle where from a rotating access point (AP) placed on the blade

of a rotating object; the RSSs are received to the station (STA) at different angles positioned at the wall in a room. For this, two modules are used as AP and STA. First, the angle between the STA and the center of rotating object is calculated. Then using the intersection between two base circles made by the angels, the distance between the wall and the center of the rotating object is calculated.

Chapter 4 has proposed a distance estimation technique between two devices based on RSSIs in different environments. With NodeMCU (ESP8266), the distances between AP and STA are measured through a straight line in the outdoor, corridor, and indoor by keeping these devices on the floor. To observe the change in RSSIs, the mean and SD-based approach is used. Besides, the curve fitting technique (CFT) is used to improve the accuracy of the estimated model. The proposed model is compared with different existing models to observe the performance accuracy. It is observed that the proposed estimation technique achieves higher accuracy compared to others.

In chapter 5, we have proposed the smartphone localization method using traditional Wi-Fi routers where three routers are placed in two rooms. The floor is divided by a grid, and using three routers' RSSI values, the smartphone positions are localized. In this process, the RSSIs values of three routers are received to the smartphone, which is forwarded to a data observing platform for analysis to produce the results. Even different special RSSI values are compared to find a suitable one. Besides, a probability-based regression analysis technique (RAT) strategy is considered. Experimental shows that the performance of the proposed method outperforms the existing methods.

Chapter 6 proposes a position-tracking technique for on-road vehicles using the RSS values to the base stations (BSs). For the this, two modules were used, one as AP and another as STA. The vehicle transmits the RSSs, and with the change of two consecutive RSSs to the BSs, its position is tracked. To track the position, the path loss model (PLM) is used, where between the intersection of multiple BSs coverages, the current location of each vehicle will be tracked. The proposed approach is highly efficient, simple and robust.

Chapter 7 has developed a sensing-capable strongly connected multi-hop router

network infrastructure for surveillance systems. In each multi-hop router, there have an AP, an STA, and a controller where wemos D1 R2 ESP8266 modules are used as AP and STA, and an Arduino Uno board is utilized as a controller. To this controller, various sensors and relays are connected. Moreover, the AP and STA are used to communicate wirelessly with other routers. Inside a router, both modules are wire connected to each other by suitable protocols. This could be helpful for several uses.

8.2 Future Scopes

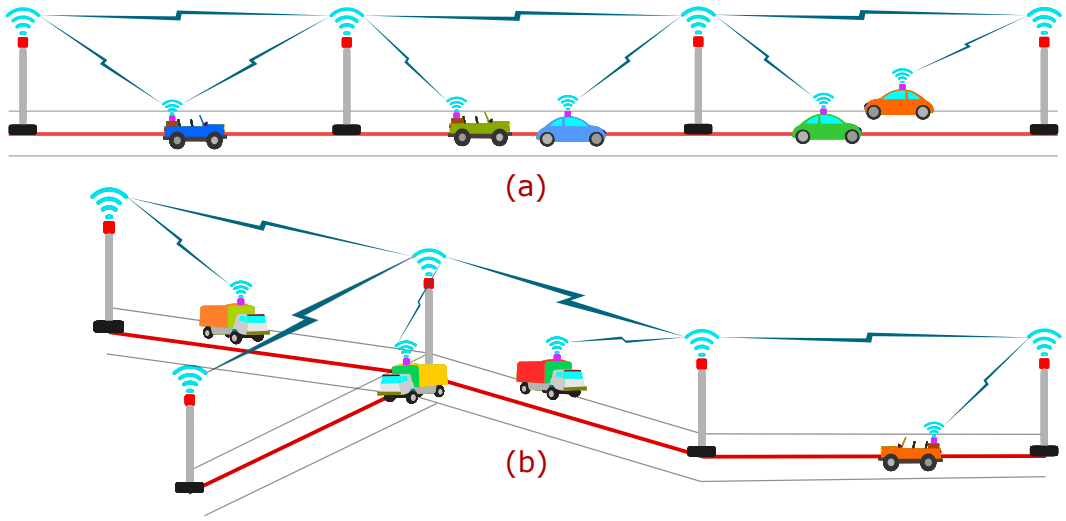

Figure 8.1: Autonomous self-driving vehicular network.

The proposed works can be used in various fields of applications like human activity recognition, traffic trajectory detection, indoor surveillance systems, smart city development, etc.

In the near future, automation technology will become an essential part of our daily life, where every wireless electronic device will be controlled through computing and sensing. Even most of the devices will be connected to each other via IoT architecture. Our next goal is to develop vehicular communications, monitoring, and control systems utilizing autonomous technologies. In this system, the wireless base station (BS), situated on the road, will be connected to

each other via a multi-hop network topology. Moreover, with these connections, not only will the vehicle be controlled, but also the passengers of these vehicles will be communicated with others. As well as, the on-road traffic monitoring system will be developed beyond these communication systems to reduce traffic jams. We also have another future plan to utilize multi-hop communication for industrial automation. These technologies are thought to consider future smart cities. Therefore, those technologies have huge demands for future hassle-free transportation architecture.

Bibliography

[1] Mohamed Ali, Mona Erfani Joorabchi, and Ali Mesbah. Same app, different app stores: A comparative study. In *2017 IEEE/ACM 4th International Conference on Mobile Software Engineering and Systems (MOBILESoft)*, pages 79–90, 2017. doi: 10.1109/MOBILESoft.2017.3.

[2] G Anitha, P Nirmala, S. Ramesh, M. Tamilselvi, and G. Ramkumar. A novel data communication with security enhancement using threat management scheme over wireless mobile networks. In *2022 International Conference on Advances in Computing, Communication and Applied Informatics (ACCAI)*, pages 1–6, 2022. doi: 10.1109/ACCAI53970.2022.9752584.

[3] Gowrish B., Siva Reddy D., A. V. G. Subramanyam, V. Senthil Kumar, and V. V. Srinivasan. Mono-pulse comparator in rectangular co-axial guide for satellite ground station. *IEEE Microwave and Wireless Components Letters*, 26(9):666–668, 2016. doi: 10.1109/LMWC.2016.2597186.

[4] Aman Batra, Mohammed El-Absi, Michael Wiemeler, Diana Gohringer, and Thomas Kaiser. Indoor thz sar trajectory deviations effects and compensation with passive sub-mm localization system. *IEEE Access*, 8: 177519–177533, 2020. doi: 10.1109/ACCESS.2020.3026884.

[5] Arne Bochem and Hang Zhang. Robustness enhanced sensor assisted monte carlo localization for wireless sensor networks and the internet of things. *IEEE Access*, 10:33408–33420, 2022. doi: 10.1109/ACCESS.2022.3162288.

[6] G. Bolotin. Space-cube: a flexible computer architecture based on stacked

modules. In *Proceedings 1996 IEEE Multi-Chip Module Conference (Cat. No.96CH35893)*, pages 20–25, 1996. doi: 10.1109/MCMC.1996.510763.

[7] S. G Briceno Muro, R. Chaparro SÃ¡nchez, and J. A. Romero Gonzalez. Digital analog conversion with spi protocol for gas sensors. In *2018 7th International Conference On Software Process Improvement (CIMPS)*, pages 131–138, 2018. doi: 10.1109/CIMPS.2018.8625626.

[8] Loredana-Maria Burciu, Radu-Petru Fotescu, Rodica-Claudia Constantinescu, Paul Svasta, and Madalin Moise. Analysis of the degree of congestion of wifi, bluetooth and zigbee communication media. In *2022 IEEE 9th Electronics System-Integration Technology Conference (ESTC)*, pages 614–617, 2022. doi: 10.1109/ESTC55720.2022.9939381.

[9] Woo Jin Byun and Yong Heui Cho. Analysis of a 200-ghz oam radio link using a generalized friis transmission equation. In *2019 IEEE International Symposium on Antennas and Propagation and USNC-URSI Radio Science Meeting*, pages 1051–1052, 2019. doi: 10.1109/APUSNCURSINRSM.2019.8888820.

[10] Marco L. Carrera, Stephane Belair, Bernard Bilodeau, Maria Abrahamowicz, Nasim Alavi, Albert Russell, and Xihong Wang. Assimilation of smap brightness temperatures in environment and climate change canada's new land surface parameterization scheme. In *2017 IEEE International Geoscience and Remote Sensing Symposium (IGARSS)*, pages 1589–1592, 2017. doi: 10.1109/IGARSS.2017.8127275.

[11] Bo Chang, Wei Tang, Xiaoyu Yan, Xin Tong, and Zhi Chen. Integrated scheduling of sensing, communication, and control for mmwave/thz communications in cellular connected uav networks. *IEEE Journal on Selected Areas in Communications*, 40(7):2103–2113, 2022. doi: 10.1109/JSAC.2022.3157366.

[12] Michael Cheffena and Marshed Mohamed. Empirical path loss models for wireless sensor network deployment in snowy environments. *IEEE*

Antennas and Wireless Propagation Letters, 16:2877–2880, 2017. doi: 10.1109/LAWP.2017.2751079.

[13] Chung-Yuan Chen, Alexander I-Chi Lai, Pei-Yuan Wu, and Ruey-Beei Wu. Optimization and evaluation of multidetector deep neural network for high-accuracy wi-fi fingerprint positioning. *IEEE Internet of Things Journal*, 9 (16):15204–15214, 2022. doi: 10.1109/JIOT.2022.3147644.

[14] Yongrui Chen, Fei Qin, and Weidong Yi. Guard beacon: An energy-efficient beacon strategy for time synchronization in wireless sensor networks. *IEEE Communications Letters*, 18(6):987–990, 2014. doi: 10.1109/LCOMM.2014.2323315.

[15] Kwan-Wu Chin, Luyao Wang, and Sieteng Soh. Joint routing and links scheduling in two-tier multi-hop rf-energy harvesting networks. *IEEE Communications Letters*, 20(9):1864–1867, 2016. doi: 10.1109/LCOMM.2016.2590463.

[16] Youngsu Cho, Myungin Ji, Yangkoo Lee, and Sangjoon Park. Wifi ap position estimation using contribution from heterogeneous mobile devices. In *Proceedings of the 2012 IEEE/ION Position, Location and Navigation Symposium*, pages 562–567, 2012. doi: 10.1109/PLANS.2012.6236928.

[17] Liangze Cui, Yao Zhang, Runren Zhang, and Qing Huo Liu. A modified efficient knn method for antenna optimization and design. *IEEE Transactions on Antennas and Propagation*, 68(10):6858–6866, 2020. doi: 10.1109/TAP.2020.3001743.

[18] J. Pacheco de Carvalho, H. Veiga, C. Pacheco, and A. Reis. A new performance assessment of 5 ghz ieee 802.11n four-node point-to-multipoint links. In *2017 11th International Conference on Measurement*, pages 159–162, 2017. doi: 10.23919/MEASUREMENT.2017.7983560.

[19] R. Diversi, R. Guidorzi, and U. Soverini. Kalman filtering in extended noise environments. *IEEE Transactions on Automatic Control*, 50(9):1396–1402, 2005. doi: 10.1109/TAC.2005.854627.

[20] Petar Djukic and Shahrokh Valaee. Delay aware link scheduling for multi-hop tdma wireless networks. *IEEE/ACM Transactions on Networking*, 17 (3):870–883, 2009. doi: 10.1109/TNET.2008.2005219.

[21] Runnan Dong, Shi Liu, Geng Liang, Xin An, and Yuanyuan Xu. Output control method of microgrid vsi control network based on dynamic matrix control algorithm. *IEEE Access*, 7:158459–158480, 2019. doi: 10.1109/ACCESS.2019.2949909.

[22] Hayat Doukkali, Sebastien Houcke, and Loutfi Nuaymi. A cross layer approach with csma/ca based protocol and cdma transmission for underwater acoustic networks. In *2007 IEEE 18th International Symposium on Personal, Indoor and Mobile Radio Communications*, pages 1–5, 2007. doi: 10.1109/PIMRC.2007.4394663.

[23] Riham Elhabyan, Wei Shi, and Marc St-Hilaire. Coverage protocols for wireless sensor networks: Review and future directions. *Journal of Communications and Networks*, 21(1):45–60, 2019. doi: 10.1109/JCN.2019.000005.

[24] Weike Feng, Jean-Michel Friedt, Gwenhael Goavec-Merou, and Motoyuki Sato. Passive radar delay and angle of arrival measurements of multiple acoustic delay lines used as passive sensors. *IEEE Sensors Journal*, 19(2): 594–602, 2019. doi: 10.1109/JSEN.2018.2872867.

[25] FabiÃ¡n Frommel, GermÃ¡n Capdehourat, and Benigno RodrÃguez. Performance analysis of wi-fi networks based on ieee 802.11ax and the coexistence with legacy ieee 802.11n standard. In *2021 IEEE URUCON*, pages 492–495, 2021. doi: 10.1109/URUCON53396.2021.9647207.

[26] Shu Fu, Hong Wen, Jinsong Wu, and Bin Wu. Cross-networks energy efficiency tradeoff: From wired networks to wireless networks. *IEEE Access*, 5:15–26, 2017. doi: 10.1109/ACCESS.2016.2585221.

[27] Damian Grzechca, Tomasz Wrobel, and Patryk Bielecki. Indoor location and idetification of objects with video survillance system and wifi module.

In *2014 International Conference on Mathematics and Computers in Sciences and in Industry*, pages 171–174, 2014. doi: 10.1109/MCSI.2014.52.

[28] Xu Guanlei, Wang Xiaotong, and Xu Xiaogang. On uncertainty principle for the linear canonical transform of complex signals. *IEEE Transactions on Signal Processing*, 58(9):4916–4918, 2010. doi: 10.1109/TSP.2010.2050201.

[29] Jiaju Guo, Haoli Zhang, Xin Liu, Dezhong Zhou, and Yanqing Hou. Oppo reno5pro smartphone single-frequency gnss positioning performance evaluation. In *2022 IEEE International Conference on Unmanned Systems (ICUS)*, pages 1415–1419, 2022. doi: 10.1109/ICUS55513.2022.9986642.

[30] Marlo Haering, Muneera Bano, Didar Zowghi, Matthew Kearney, and Walid Maalej. Automating the evaluation of education apps with app store data. *IEEE Transactions on Learning Technologies*, 14(1):16–27, 2021. doi: 10.1109/TLT.2021.3055121.

[31] Ji Haoran, Sun Liang Kai, Yu Hong, Yang Pingyi, and Liang Chen. A new method for fault location considering primary/secondary disconnection. In *2021 International Conference on Control Science and Electric Power Systems (CSEPS)*, pages 257–261, 2021. doi: 10.1109/CSEPS53726.2021.00058.

[32] Shiming He, Kun Xie, Weiwei Chen, Dafang Zhang, and Jigang Wen. Energy-aware routing for swipt in multi-hop energy-constrained wireless network. *IEEE Access*, 6:17996–18008, 2018. doi: 10.1109/ACCESS.2018.2820093.

[33] Minh Tu Hoang, Yizhou Zhu, Brosnan Yuen, Tyler Reese, Xiaodai Dong, Tao Lu, Robert Westendorp, and Michael Xie. A soft range limited k-nearest neighbors algorithm for indoor localization enhancement. *IEEE Sensors Journal*, 18(24):10208–10216, 2018. doi: 10.1109/JSEN.2018.2874453.

[34] Rick C. J. Hsu, Ali Ayazi, Bijan Houshmand, and Bahram Jalali. All-

dielectric wireless receiver. In *2007 IEEE/MTT-S International Microwave Symposium*, pages 221–224, 2007. doi: 10.1109/MWSYM.2007.380367.

[35] Yi Huang and Wenbin Liu. Regression analysis model based on data processing and matlab numerical simulation. In *2022 IEEE Asia-Pacific Conference on Image Processing, Electronics and Computers (IPEC)*, pages 1115–1118, 2022. doi: 10.1109/IPEC54454.2022.9777319.

[36] Arshad Iqbal, Yunmin Kim, and Tae-Jin Lee. Access mechanism in wireless powered communication networks with harvesting access point. *IEEE Access*, 6:37556–37567, 2018. doi: 10.1109/ACCESS.2018.2851941.

[37] Xueqin Jiang and Moon Ho Lee. Large girth non-binary ldpc codes based on finite fields and euclidean geometries. *IEEE Signal Processing Letters*, 16(6):521–524, 2009. doi: 10.1109/LSP.2009.2016830.

[38] Satish R. Jondhale and Rajkumar S. Deshpande. Kalman filtering framework-based real time target tracking in wireless sensor networks using generalized regression neural networks. *IEEE Sensors Journal*, 19(1): 224–233, 2019. doi: 10.1109/JSEN.2018.2873357.

[39] Lia Kamelia, Susanto Nugraha, Mufid Ridlo Effendi, and Setia Gumilar. Real-time monitoring system for measurement of soil fertility parameters in smart farming applications. In *2019 IEEE 5th International Conference on Wireless and Telematics (ICWT)*, pages 1–4, 2019. doi: 10.1109/ICWT47785.2019.8978268.

[40] A. S. Keerthi Nayani, G. Nikhilesh, and S. Shiva Tej Kumar. Design and implementation of uart protocol for avionics applications. In *2019 International Conference on Intelligent Computing and Control Systems (ICCS)*, pages 1402–1407, 2019. doi: 10.1109/ICCS45141.2019.9065366.

[41] Taehyoun Kim, Samjoon Park, and Taeho Lee. Applying software reliability engineering process to software development in korea defense industry. In *2017 IEEE International Symposium on Software Reliability Engineering Workshops (ISSREW)*, pages 81–81, 2017. doi: 10.1109/ISSREW.2017.26.

[42] Kyungmin Kwak, Daegil Park, Wan Kyun Chung, and Jinhyun Kim. Underwater 3-d spatial attenuation characteristics of electromagnetic waves with omnidirectional antenna. *IEEE/ASME Transactions on Mechatronics*, 21(3):1409–1419, 2016. doi: 10.1109/TMECH.2015.2509466.

[43] Minhae Kwon, Juhyeon Lee, and Hyunggon Park. Intelligent iot connectivity: Deep reinforcement learning approach. *IEEE Sensors Journal*, 20(5): 2782–2791, 2020. doi: 10.1109/JSEN.2019.2949997.

[44] L. Chang L. Li and F. Song. A smart collaborative routing protocol for qoe enhancement in multi-hop wireless networks. *IEEE Access*, 8:100963–100973, 2020. doi: 10.1109/ACCESS.2020.2820093.

[45] Athanasios E. Lagias, Thomas D. Lagkas, and Jie Zhang. New rssi-based tracking for following mobile targets using the law of cosines. *IEEE Wireless Communications Letters*, 7(3):392–395, 2018. doi: 10.1109/LWC.2017.2779507.

[46] C.C. Landinger, J.W. McAuliffe, A.L. Clapp, J.B. Dagenhart, and W.A. Thue. Safety considerations of aerial systems using insulated and covered wire and cable. *IEEE Transactions on Power Delivery*, 12(2):1012–1016, 1997. doi: 10.1109/61.584430.

[47] Binghao Li, Kai Zhao, and Xuesong Shen. Dilution of precision in positioning systems using both angle of arrival and time of arrival measurements. *IEEE Access*, 8:192506–192516, 2020. doi: 10.1109/ACCESS.2020.3033281.

[48] Hongran Li and Shigeru Yamamoto. Polynomial regression based model-free predictive control for nonlinear systems. In *2016 55th Annual Conference of the Society of Instrument and Control Engineers of Japan (SICE)*, pages 578–582, 2016. doi: 10.1109/SICE.2016.7749264.

[49] Hongwei Li, Chao Li, Hang Gao, Shiyou Wu, and Guangyou Fang. Study of moving targets tracking methods for a multi-beam tracking system in terahertz band. *IEEE Sensors Journal*, 21(5):6520–6529, 2021. doi: 10.1109/JSEN.2020.3041363.

[50] Lianlin Li, Wenji Zhang, and Fang Li. Tomographic reconstruction using the distorted rytov iterative method with phaseless data. *IEEE Geoscience and Remote Sensing Letters*, 5(3):479–483, 2008. doi: 10.1109/LGRS.2008.919818.

[51] Chih-Lung Lin, Yi-Ming Chang, Hung-Sheng Chen, Cheng-Yan Chuang, and Ting-Ching Chu. Position tracking based on particle filter for self-capacitance single-touch screen panels. *Journal of Display Technology*, 11 (2):165–169, 2015. doi: 10.1109/JDT.2014.2363296.

[52] Ruikai Mai, Duy H. N. Nguyen, and Tho Le-Ngoc. Linear precoding game for mimo mac with dynamic access point selection. *IEEE Wireless Communications Letters*, 4(2):153–156, 2015. doi: 10.1109/LWC.2014.2387833.

[53] F. Morales, Ll. Gifre, F. Paolucci, M. Ruiz, F. Cugini, P. Castoldi, and L. Velasco. Dynamic core vnt adaptability based on predictive metro-flow traffic models. *Journal of Optical Communications and Networking*, 9(12): 1202–1211, 2017. doi: 10.1364/JOCN.9.001202.

[54] H. Nonaka and Tsutomu Da-te. Ultrasonic position measurement and its applications to human interface. *IEEE Transactions on Instrumentation and Measurement*, 44(3):771–774, 1995. doi: 10.1109/19.387329.

[55] Mayu Ohtani, Hisato Iwai, and Hideichi Sasaoka. Improvement of position estimation accuracy using multiple access points in terminal position estimation based on position fingerprint. In *2014 International Symposium on Antennas and Propagation Conference Proceedings*, pages 399–400, 2014. doi: 10.1109/ISANP.2014.7026698.

[56] Shaoming Pan, Yulong Tao, Congchong Nie, and Yanwen Chong. Pegnet: Progressive edge guidance network for semantic segmentation of remote sensing images. *IEEE Geoscience and Remote Sensing Letters*, 18(4):637–641, 2021. doi: 10.1109/LGRS.2020.2983464.

[57] Sweta V Parvati, K. Thenmozhi, Padmapriya Praveenkumar, S Sathish, and Rengarajan Amirtharajan. Iot accelerated wi-fi bot controlled via node

mcu. In *2018 International Conference on Computer Communication and Informatics (ICCCI)*, pages 1–3, 2018. doi: 10.1109/ICCCI.2018.8441215.

[58] Norasage Pattanadech and Peerawut Yutthagowith. Fast curve fitting algorithm for parameter evaluation in lightning impulse test technique. *IEEE Transactions on Dielectrics and Electrical Insulation*, 22(5):2931–2936, 2015. doi: 10.1109/TDEI.2015.005165.

[59] Panaya Pengboon and Pasu Kaewplung. An efficient algorithm for designing multi-hop wireless connections for wireless-optical broadband access network. In *2012 21st Annual Wireless and Optical Communications Conference (WOCC)*, pages 163–165, 2012. doi: 10.1109/WOCC.2012.6198175.

[60] M. PremKumar, S. Edwin Chandra, M. AshokRaj, and M. Grace Prasana. Digital signal processing issues for wireless communication systems in line of sight(los) and non line of sight (nlos) environments. In *2016 International Conference on Circuit, Power and Computing Technologies (ICCPCT)*, pages 1–5, 2016. doi: 10.1109/ICCPCT.2016.7530141.

[61] Puli Dilliswar Reddy and L. Rama Parvathy. Prediction analysis using random forest algorithms to forecast the air pollution level in a particular location. In *2022 3rd International Conference on Smart Electronics and Communication (ICOSEC)*, pages 1585–1589, 2022. doi: 10.1109/ICOSEC54921.2022.9952138.

[62] Christopher Rose, Jordan Britt, John Allen, and David Bevly. An integrated vehicle navigation system utilizing lane-detection and lateral position estimation systems in difficult environments for gps. *IEEE Transactions on Intelligent Transportation Systems*, 15(6):2615–2629, 2014. doi: 10.1109/TITS.2014.2321108.

[63] Hazem Sallouha, Mohammad Mahdi Azari, Alessandro Chiumento, and Sofie Pollin. Aerial anchors positioning for reliable rss-based outdoor localization in urban environments. *IEEE Wireless Communications Letters*, 7 (3):376–379, 2018. doi: 10.1109/LWC.2017.2778723.

[64] Wang Sansheng, Zhang Mingji, Zhang Ning, and Guo Qiang. Calculation and correction of magnetic object positioning error caused by magnetic field gradient tensor measurement. *Journal of Systems Engineering and Electronics*, 29(3):456–461, 2018. doi: 10.21629/JSEE.2018.03.02.

[65] Roshmi Sarmah, Manasjyoti Bhuyan, and Monowar H. Bhuyan. Sure-h: A secure iot enabled smart home system. In *2019 IEEE 5th World Forum on Internet of Things (WF-IoT)*, pages 59–63, 2019. doi: 10.1109/WF-IoT.2019.8767229.

[66] Christopher G. Scully, Jinseok Lee, Joseph Meyer, Alexander M. Gorbach, Domhnull Granquist-Fraser, Yitzhak Mendelson, and Ki H. Chon. Physiological parameter monitoring from optical recordings with a mobile phone. *IEEE Transactions on Biomedical Engineering*, 59(2):303–306, 2012. doi: 10.1109/TBME.2011.2163157.

[67] Sihua Shao, Abdallah Khreishah, Moussa Ayyash, Michael B. Rahaim, Hany Elgala, Volker Jungnickel, Dominic Schulz, Thomas D.C. Little, Jonas Hilt, and Ronald Freund. Design and analysis of a visible-light-communication enhanced wifi system. *Journal of Optical Communications and Networking*, 7(10):960–973, 2015. doi: 10.1364/JOCN.7.000960.

[68] Surinder Singh. Performance comparison of optical network topologies in the presence of optimized semiconductor optical amplifiers. *Journal of Optical Communications and Networking*, 1(4):313–323, 2009. doi: 10.1364/JOCN.1.000313.

[69] I. Sletbak, R. Kristensen, H. Sundklakk, G. Navik, and M. Runde. Glowing contact areas in loose copper wire connections. In *Electrical Contacts - 1991 Proceedings of the Thirty-Seventh IEEE HOLM Conference on Electrical Contacts*, pages 244–248, 1991. doi: 10.1109/HOLM.1991.170830.

[70] S. H. Song, Marco Antonelli, Tony W. K. Fung, Brandon D. Armstrong, Amy Chong, Albert Lo, and Bertram E. Shi. Developing and assessing matlab exercises for active concept learning. *IEEE Transactions on Education*, 62(1):2–10, 2019. doi: 10.1109/TE.2018.2811406.

[71] Dongeun Suh, Haneul Ko, and Sangheon Pack. Efficiency analysis of wifi offloading techniques. *IEEE Transactions on Vehicular Technology*, 65(5): 3813–3817, 2016. doi: 10.1109/TVT.2015.2437325.

[72] Zhiguo Sun, Kaixuan Wang, Rongchen Sun, and Zengmao Chen. Channel state identification in complex indoor environments with st-cnn and transfer learning. *IEEE Communications Letters*, 27(2):546–550, 2023. doi: 10.1109/LCOMM.2022.3220506.

[73] Dvijen Trivedi, Aniruddha Khade, Kashish Jain, and Ruchira Jadhav. Spi to i2c protocol conversion using verilog. In *2018 Fourth International Conference on Computing Communication Control and Automation (ICCUBEA)*, pages 1–4, 2018. doi: 10.1109/ICCUBEA.2018.8697415.

[74] Anand V. Varma, P.S. Random forest learning based indoor localization as an iot service for smart buildings. *Wireless Pers Commun*, 117:3209â3227, 2021. doi: org/10.1007/s11277-020-07977-w.

[75] Anatolyy Vlasyuk, Viktor Zhukovskyy, Nataliia Zhukovska, and Hesham Rajab. One-dimensional modeling of contaminant migration in unsaturated porous media with dispersed catalyst particles. In *2020 International Conference on Mathematics and Computers in Science and Engineering (MACISE)*, pages 197–201, 2020. doi: 10.1109/MACISE49704.2020.00043.

[76] Dawei Wang, Pinyi Ren, Qinghe Du, Li Sun, and Yichen Wang. Security provisioning for miso vehicular relay networks via cooperative jamming and signal superposition. *IEEE Transactions on Vehicular Technology*, 66(12): 10732–10747, 2017. doi: 10.1109/TVT.2017.2703780.

[77] Huan Wang, Kaiping Xue, Peilin Hong, and Hancheng Lu. Impact of traffic pattern on benefits of practical multi-hop network coding in wireless networks. In *2011 IEEE Consumer Communications and Networking Conference (CCNC)*, pages 1197–1201, 2011. doi: 10.1109/CCNC.2011.5766432.

[78] Hui-Ming Wang, Yan Zhang, Xu Zhang, and Zhetao Li. Secrecy and covert communications against uav surveillance via multi-hop net-

works. *IEEE Transactions on Communications*, 68(1):389–401, 2020. doi: 10.1109/TCOMM.2019.2950940.

[79] Wei Wang, Xuming Liu, Maozhen Li, Zhaoba Wang, and Cunhua Wang. Optimizing node localization in wireless sensor networks based on received signal strength indicator. *IEEE Access*, 7:73880–73889, 2019. doi: 10.1109/ACCESS.2019.2920279.

[80] Ran Wei and Justin Zhan. Improved customers' privacy preference policy. In *2007 IEEE International Conference on Granular Computing (GRC 2007)*, pages 787–787, 2007. doi: 10.1109/GrC.2007.129.

[81] Fei Wu, Jian Xing, and Bo Dong. An indoor localization method based on rssi of adjustable power wifi router. In *2015 Fifth International Conference on Instrumentation and Measurement, Computer, Communication and Control (IMCCC)*, pages 1481–1484, 2015. doi: 10.1109/IMCCC.2015.313.

[82] Yaqin Xie, Yan Wang, Arumugam Nallanathan, and Lina Wang. An improved k-nearest-neighbor indoor localization method based on spearman distance. *IEEE Signal Processing Letters*, 23(3):351–355, 2016. doi: 10.1109/LSP.2016.2519607.

[83] Shibo Xin, Yali Wang, and Wenqing Lv. Standard deviation control chart based on weighted standard deviation method. In *Proceedings of the 33rd Chinese Control Conference*, pages 3574–3579, 2014. doi: 10.1109/ChiCC.2014.6895533.

[84] Li Xu, Ling-Juan Miao, and Jun Shen. Optimal design of the serial data receiving path. In *Proceedings of the 30th Chinese Control Conference*, pages 4469–4474, 2011.

[85] Weixing Xue, Qingquan Li, Xianghong Hua, Kegen Yu, Weining Qiu, and Baoding Zhou. A new algorithm for indoor rssi radio map reconstruction. *IEEE Access*, 6:76118–76125, 2018. doi: 10.1109/ACCESS.2018.2882379.

[86] Kuo Yang, Zhonghua Liang, Ren Liu, and Wei Li. Rss-based indoor localization using min-max algorithm with area partition strategy. *IEEE Access*, 9:125561–125568, 2021. doi: 10.1109/ACCESS.2021.3111650.

[87] Serhiy Yefimenko and Volodymyr Stepashko. Revised successive search gmdh algorithm with recurrent estimating model parameters. In *2019 IEEE 14th International Conference on Computer Sciences and Information Technologies (CSIT)*, volume 1, pages 191–194, 2019. doi: 10.1109/STC-CSIT.2019.8929866.

[88] Wang Q. Zhang H. et al. Yin, Y. Novel distributed sensor fusion algorithm for rssi-based location estimation using the unscented kalman filter. *Wireless Pers Commun*, 117:607â621, 2021. doi: org/10.1007/s11277-020-07888-w.

[89] Jaehyun Yoo. Change detection of rssi fingerprint pattern for indoor positioning system. *IEEE Sensors Journal*, 20(5):2608–2615, 2020. doi: 10.1109/JSEN.2019.2951712.

[90] Hyun-Jae Yoon, Nack-Jin Chung, Min-Ho Choi, In-Shik Park, and Jichai Jeong. Estimation of system reliability for uncooled optical transmitters using system reliability function. *Journal of Lightwave Technology*, 17(6): 1067–1071, 1999. doi: 10.1109/50.769309.

[91] Lixia Zhang, Yang Li, Bijie Qiu, Jianliang Zhang, and Weiwei Liang. Design of communication power centralized remote monitoring system based on big data technology. In *2021 International Conference on Electronics, Circuits and Information Engineering (ECIE)*, pages 46–49, 2021. doi: 10.1109/ECIE52353.2021.00017.

[92] Shichao Zhang, Xuelong Li, Ming Zong, Xiaofeng Zhu, and Ruili Wang. Efficient knn classification with different numbers of nearest neighbors. *IEEE Transactions on Neural Networks and Learning Systems*, 29(5):1774–1785, 2018. doi: 10.1109/TNNLS.2017.2673241.

[93] Yongqiang Zhang, Liangliang Li, and Yongjian Zhang. Research and design of location tracking system used in underground mine based on wifi technology. In *2009 International Forum on Computer Science-Technology and Applications*, volume 3, pages 417–419, 2009. doi: 10.1109/IFCSTA.2009.341.

[94] Zhiwei Zhang, Ao Sun, Xu Zhang, Dan Zhang, and Zhisheng Li. Optimal placement of base stations in falling point measurement at sea. In *2020 5th International Conference on Automation, Control and Robotics Engineering (CACRE)*, pages 468–472, 2020. doi: 10.1109/CACRE50138.2020.9230350.

[95] Zhonghua Zhang and Di Chen. An improved rssi-based centroid localization algorithm in wireless sensor networks. In *2011 International Conference on Computer Science and Service System (CSSS)*, pages 3008–3011, 2011. doi: 10.1109/CSSS.2011.5972162.

[96] Cheng Zhao, Wuxiong Zhang, Yang Yang, and Sha Yao. Treelet based clustered compressive data aggregation for wireless sensor networks. *IEEE Transactions on Vehicular Technology*, 64(9):4257–4267, 2015. doi: 10.1109/TVT.2014.2361250.

[97] Yuan J. Liu H. et al. Zhou, C. Bluetooth indoor positioning based on rssi and kalman filter. *Wireless Pers Commun*, 96:4115â4130, 2017. doi: org/10.1007/s11277-017-4371-4.

[98] Zhiwen Zhu, Wenbing Guan, Linfeng Liu, Sheng Li, Shanshan Kong, and Yudao Yan. A multi-hop localization algorithm in underwater wireless sensor networks. In *2014 Sixth International Conference on Wireless Communications and Signal Processing (WCSP)*, pages 1–6, 2014. doi: 10.1109/WCSP.2014.6992019.

[99] Aleksey V. Zinkevich. Esp8266 microcontroller application in wireless synchronization tasks. In *2021 International Conference on Industrial Engineering, Applications and Manufacturing (ICIEAM)*, pages 670–674, 2021. doi: 10.1109/ICIEAM51226.2021.9446411.

[100] Samuele Zoppi, Amaury Van Bemten, H. Murat GÃ¼rsu, Mikhail Vilgelm, Jochen Guck, and Wolfgang Kellerer. Achieving hybrid wired/wireless industrial networks with wdetserv: Reliability-based scheduling for delay guarantees. *IEEE Transactions on Industrial Informatics*, 14(5):2307–2319, 2018. doi: 10.1109/TII.2018.2803122.

Index

Published works included in this thesis:

1. Suvankar Barai, Debajyoti Biswas and Buddhadeb Sau, *Improved RSSI based Angle Localization using Rotational Object*, 2020 International Conference on Power Electronics and Renewable Energy Applications (PEREA), Kannur, India, 2020, pp. 1-5, doi: 10.1109/PEREA51218.2020.9339773.

2. Debajyoti Biswas, Suvankar Barai and Buddhadeb Sau, *Reliable RSSI Trend based Localization for three Different Environments*, 2020 2nd International Conference on Advances in Computing, Communication Control and Networking (ICACCCN), Greater Noida, India, 2020, pp. 381-386, doi: 10.1109 /ICACCCN51052.2020.9362961.

3. Debajyoti Biswas, Suvankar Barai and Buddhadeb Sau, *Enhanced RSSI-Based Real-Time Position-Tracking System in Vehicular Networks*, in IEEE Sensors Letters, vol. 6, no. 6, pp. 1-4, June 2022, Art no. 7500604, doi: 10.1109/LSENS.2022.3173706.

4. Debajyoti Biswas, Suvankar Barai and Buddhadeb Sau, *New RSSI-Fingerprinting-Based Smartphone Localization System For Indoor Environments*, in Wireless Networks (2022). https://doi.org/10.1007/s11276-022-03188-2.

5. Debajyoti Biswas, Suvankar Barai and Buddhadeb Sau, *A WiFi-based Self-Organizing Multi-Hop Sensor Network for Internet of Things*, 2021 International Conference on Innovative Trends in Information Technology (ICITIIT), Kottayam, India, 2021, pp. 1-6, doi: 10.1109/ICITIIT5152.

Published works not included in this thesis:

6. Suvankar Barai, Debajyoti Biswas and Buddhadeb Sau, *Estimate Distance Measurement using NodeMCU ESP8266 based on RSSI Technique*. The proceedings of IEEE Conference on Antenna Measurements & Applications (CAMA), 4-6 December 2017, Tsukuba, Japan, pp. 170-173, ISBN: 978-1-5090-5028-4.

7. Suvankar Barai, Debajyoti Biswas and Buddhadeb Sau, *Sensors Positioning for Reliable RSSI-based Outdoor Localization using CFT*, 2020 IEEE International Symposium on Sustainable Energy, Signal Processing and Cyber Security (iSSSC), Gunupur Odisha, India, 2020, pp. 1-5, doi: 10.1109/iSSSC50941.2020.9358844.

8. Debajyoti Biswas, Suvankar Barai and Buddhadeb Sau, *Improved RSSI based Vehicle Localization using Base Station*, 2021 International Conference on Innovative Trends in Information Technology (ICITIIT), Kottayam, India, 2021, pp. 1-6, doi: 10.1109/ICITIIT51526.2021.9399596.

9. Debajyoti Biswas, Suvankar Barai, Buddhadeb Sau, *Advanced RSSI-Based Wi-Fi Access Point Localization Using Smartphone*, Innovations in Electrical and Electronic Engineering. Lecture Notes in Electrical Engineering, 756. Springer, Singapore. https://doi.org/10.1007/978-981-16-0749-3_42.